

King Saud University

College of Engineering

Petroleum and Natural Gas Engineering Department



Experimental Investigation of CO₂ - Miscible Oil Recovery at Different Conditions

By

Ali Suleman Al-Netaifi

A Thesis Submitted in Partial Fulfillment of the Requirement of the Degree of Master of Science in the Department of Petroleum and Natural Gas Engineering

**The graduate School
King Saud University**

**Rajb, 1429 H.
July, 2008 G.**

We hereby approve the thesis entitled:

“Experimental Investigation of CO₂ - Miscible Oil Recovery at Different Conditions”

Prepared by:

ENGINEER: ALI SULEMAN AL-NETAIFI

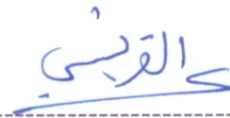
Committee Members:

Advisor



Dr. EISSA M. SHOKIR

Co-advisor



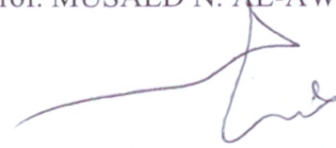
Dr. ABDULRAHMAN AL-QURAIISHI

Examiner



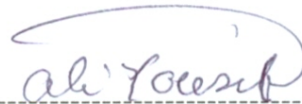
Prof. MUSAED N. AL-AWAD

Examiner



Dr. ALI A. AL-MESHARI

Examiner



Dr. ALI A. AL-YOUSIF

ACKNOWLEDGMENT

I thank Almighty God for giving me the help, strength and towards accomplishing all my academics endeavors and realizing my personal dreams.

I would like to thank my supervisor, and mentor Dr. Eissa Mohamed Shokir for giving me an opportunity to be on his team. My deepest appreciation for his motivation, guidance, and sound advice throughout the entire program.

My thanks go also to Dr. Abdulrahman AlQuraishi (King Abdulaziz City for Science and Technology) thesis co-supervisor for his valuable guidance, comments and suggestions. I would also like to express my sincere thanks to the department faculties and colleagues for their constant encouragement and support.

The deep appreciation is further extended to the Petroleum and Natural Gas Engineering Department at King Saud University (KSU), and the Oil and Gas Centre at the King Abdulaziz City for Science and Technology (KACST) for the facilities provided and the generous financial support.

Finally, I would like to thank all members of my family, especially my parents for theirs prayers and patients. Special thanks are extended to my wife for the encouragement, and understanding.

ABSTRACT

In miscible flooding, the incremental oil recovery is obtained by one of three mechanisms. These mechanisms are oil displacement by solvent through the generation of miscibility, oil swelling, and reduction in oil viscosity.

To evaluate the performance of miscible CO₂ flooding, extensive laboratory tests were conducted on 2 and 4 ft long sandstone cores using low and high salinity brine solutions as aqueous phase and three different oleic phases (n-Decane, light, and medium Saudi crude oils). Injection scheme (Continuous Gas Injection "CGI" versus Water Alternating Gas "WAG"), WAG ratio, slug size, oil types, core orientation and core length were investigated. In addition, miscible WAG flooding as a secondary process was investigated and its efficiency was compared to the conventional tertiary miscible gas flooding.

Miscible CO₂ flooding experiments at different WAG parameters (WAG ratio and slug size) indicate that 1:2 WAG ratio at 0.2 PV slug size is the best combination delivering the highest recovery and tertiary recovery factors. Miscible WAG flooding as a secondary process was investigated and indicated a higher ultimate recovery than that obtained from the conventional tertiary WAG flooding. However, larger amount of gas injection is consumed particularly in the early stages of the injection process.

Reduction in oil recovery and tertiary recovery factor were observed with decreasing oil API for miscible WAG flooding. This is believed to be a result of wettability alteration and viscous fingering. Equal ultimate recovery was obtained for the miscible experiments conducted with different brine composition and concentration with some delay in approaching that recovery when using the low salinity brine solution. This resulted in an increase in tertiary recovery factor and slight decrease in the UF as we switch from low to high salinity brine.

Miscible WAG injection in vertically mounted core sample representing updipping reservoirs was investigated and resulted in slightly lower oil recovery compared to that obtained from horizontally laid core sample at the same conditions of WAG ratio and slug

size. Miscible WAG flooding process in different core lengths showed similar ultimate recovery factor. Small delay has been noticed in approaching the ultimate recovery for the short core sample.

Miscible CGI mode conducted using n-decane as oleic phase showed better performance in term of recovery than miscible WAG injection conducted with the same oleic phase. Berea cores used in this work are known to be strongly water wet. In addition, mineral oil, used as oleic phase, is known to be non wetting. Therefore, such observation, agrees well with the previous mentioned observation on the efficiency of CGI in water wet media. However, larger amount of gas injection is needed, therefore, economically unfeasible. When light crude oil was used as oleic phase, higher recovery was obtained for miscible WAG. The reversal trend seen in this set of experiments compared to that conducted using n-Decan is because of the presence of crude oil, which alters the rock wettability towards oil-wet condition preventing the water blockage during the WAG process.

TABLE OF CONTENTS

	<u>Page</u>
ACKNOWLEDGMENT	i
ABSTRACT	ii
TABLE OF CONTENTS	iv
LIST OF FIGURES	vi
LIST OF TABLES	ix
CHAPTER 1: INTRODUCTION	1
CHAPTER 2: LITERATURE REVIEW	3
2.1 Miscible CO ₂ Flooding	5
2.1.1 Minimum Miscibility Pressure	9
2.1.1.1 Experimental Methods	10
2.1.1.2 Mathematical Determination of MMP	13
2.2 Immiscible CO ₂ Displacement Method	19
2.3 Water Alternating Gas Injection (WAG) Process	20
2.3.1 WAG Ratio	21
2.3.2 Slug Size	22
CHAPTER 3: STATEMENT OF THE PROBLEM	25
CHAPTER 4: EXPERIMENTAL APPARATUS & PROCEDURE	26
4.1 Rocks and Fluids	26
4.2 Experimental Setup	29
4.3 Experimental Procedure	29
CHAPTER 5: RESULTS AND DISCUSSIONS	33

5.1 Effect of Slug Size	38
5.2 Effect of WAG Ratio	42
5.3 Secondary versus Tertiary WAG Injection	48
5.4 Effect of Brine Composition	51
5.5 Effect of Oil Type and Viscosity	54
5.6 Effect of Core Orientation	56
5.7 Effect of Core Length	58
5.8 CGI versus WAG Injection Mode	58
CHAPTER 6: CONCLUSIONS AND RECOMMENDATIONS	66
NOMENCLATURE	68
REFERENCES	70

LIST OF FIGURES

<u>Figure No.</u>		<u>Page</u>
2.1	Oil recovery methods sequence in a typical oilfield [15]	4
2.2	1-D Schematic of The Dynamics CO ₂ Miscible Process [16]	6
2.3	Schematic of WAG miscible CO ₂ -EOR [16]	8
2.4	Slime tube apparatus[31]	12
2.5	Schematic of the rising bubble apparatus [36]	12
2.6	Comparison of different WAG ratios in terms of the incremental oil recovery as a function of the CO ₂ slug size [66]	23
4.1	Schematic of the experimental set-up	30
5.1	Cumulative oil recovery versus cumulative water volume injected during the water flood process on run 15	35
5.2	Effect of slug size on recovery factor of 1:1 miscible WAG displacement experiments using n-Decane-brine fluid pair	39
5.3	Effect of slug size on tertiary recovery factor of miscible 1:1 WAG displacement experiments using n-Decane-brine fluid pair	39
5.4	Effect of slug size on recovery factor of miscible 1:2 WAG displacement experiments using n-Decane-brine fluid pair	41
5.5	Effect of slug size on tertiary recovery factor of miscible 1:2 WAG displacement experiments using n-Decane-brine fluid pair	41
5.6	Effect of miscible WAG ratio on recovery factor for 0.4 PV slug size displacement experiments using n-Decane-brine fluid pair	43
5.7	Effect of miscible WAG ratio on tertiary recovery factor for 0.4 PV slug size displacement experiments using n-Decane-brine fluid pair	45
5.8	Effect of miscible WAG ratio on recovery factor for 0.2 PV slug size displacement experiments using Saudi light crude synthetic formation brine fluid pair	45

5.9	Effect of miscible WAG ratio on tertiary recovery factor for 0.2 PV slug size displacement experiments using Saudi light crude-synthetic formation brine fluid pair	46
5.10	Effect of miscible WAG Parameters on recovery factor for n-Decane-brine fluid pair	46
5.11	Effect of miscible WAG Parameters on tertiary recovery factor for n-Decane-brine fluid pair	47
5.12	CO ₂ Utilization Factor, tertiary recovery factor, and recovery factor of different miscible WAG parameters for n-Decane-brine fluid pair	49
5.13	Recover factor in percentage of initial oil in place for secondary and tertiary gas injection using n-Decane-brine fluid pair	50
5.14	Tertiary recovery factor of tertiary versus secondary miscible gas injection using n-Decane-brine fluid pair	52
5.15	Effect of brine composition on n-Decane recovery factor of miscible flooding at 1:2 WAG ratio, 0.2 PV slug size	52
5.16	Effect of brine composition on n-Decane tertiary recovery factor of miscible flooding at 1:2 WAG ratio, 0.2 PV slug size	53
5.17	Effect of oil type on recovery factor of miscible flooding at 1:2 WAG ratio, 0.2 PV slug size	55
5.18	Effect of oil type on tertiary recovery factor of miscible flooding at 1:2 WAG ratio, 0.2 PV slug size	55
5.19	Effect of core orientation on recovery factor of miscible flooding at 1:2 WAG ratio, 0.2 PV slug size using Saudi light crude-synthetic formation brine fluid pair	57
5.20	Effect of core orientation on tertiary recovery factor of miscible flooding at 1:2 WAG ratio, 0.2 PV slug size using Saudi light crude-synthetic formation brine fluid pair	57
5.21	Effect of core length on recovery factor of miscible flooding at 1:2 WAG ratio, 0.2 PV slug size using Saudi light crude-	

	synthetic formation brine fluid pair	59
5.22	Effect of core length on tertiary recovery factor of miscible flooding at 1:2 WAG ratio, 0.2 PV slug size using Saudi light crude oil- synthetic formation brine fluid pair	59
5.23	Effect of miscible injection mode on recovery factor using n-Decane-brine fluid pair	61
5.24	Effect of miscible injection mode on tertiary recovery factor using n-Decane-brine fluid pair	61
5.25	CO ₂ Utilization Factor, tertiary recovery factor, and recovery factor of CGI and WAG injection mode for n-Decane-brine fluid pair	62
5.26	Effect of miscible injection mode on recovery factor using Saudi light crude-synthetic formation brine fluid pair on 4 ft long core	62
5.27	Effect of miscible injection mode on tertiary recovery factor using Saudi light crude-synthetic formation brine fluid pair on 4 ft long core	64

LIST of TABLES

<u>Table No.</u>		<u>Page</u>
2.1	Commonly used CO ₂ -Oil MMP correlations	14
4.1	Physical properties of used n-Deane and aqueous solutions	27
4.2	Properties of the Saudi Crude Oils [71]	27
4.3	Minimum miscibility pressure values of the binary oil-brine systems	28
5.1	Petrophysical properties of water flooded rock samples	34
5.2	Summery of conducted miscible gas flooding experimental runs	36

CHAPTER 1

INTRODUCTION

With the high environmental awareness, Kyoto protocol was issued to reduce the greenhouse gases (GHG) emissions including CO₂. Cement Factories, power and desalination plants, Gas flaring and CO₂ emission from natural gas processing are considered to be the main sources of CO₂ emission.

Carbon Dioxide Capture and storage in depleted or partially depleted reservoirs are perfect option for CO₂ emission reduction. This process has been first deployed in United States as a part of enhanced oil recovery (EOR) project in early 1970. Ever since, it has been ongoing practice in many other areas. Geological storage of GHG such as CO₂ gained credibility early 1990s where the first large-scale storage project was started at the Sleipner gas field in the North Sea. By the end of 1990s, a number of research programs was under way in the United States, Canada, Japan, Europe and Australia [1].

Oil companies became increasingly interested in geological storage as a mitigation option, for gas fields with a high natural CO₂ content. In Salah Gas Field in Algeria is an example project where stripped CO₂ from natural gas was re-injected into the gas reservoir outside the boundaries of the gas field. Another project is started in the Barents Sea, where stripped CO₂ is injected into a formation below the gas field. Chevron is proposing to produce gas containing about 14% CO₂ from the Gorgon field of Australia and re-inject it into the Dupuy Formation at Barrow Island [2]. In The Netherlands, CO₂ is injected at pilot scale into the partially depleted offshore gas field [3]. Similarly, forty-four small-scale CO₂-rich acid gas injection projects are currently operating in Western Canada, since the early 1990s [4]. All of these projects provide important examples of how effective are CO₂ and other greenhouse gases injection is as a mean of GHG sequestration.

Global estimates of storage capacity in oil reservoirs vary from 126 to 400 GtCO₂, including potential undiscovered reservoirs, compared to 800 GtCO₂ in gas reservoirs [5]. Practiced CO₂ flooding process today is not engineered to maximize CO₂ storage but also

to maximize revenues from oil production. This requires minimizing the amount of CO₂ retained in the reservoir. In the future, if storing CO₂ has an economic value, co-optimizing CO₂ storage and EOR may increase capacity estimates.

In United States, there are approximately 73 CO₂-EOR projects injecting up to 30 MtCO₂ annually. Most of the CO₂ are from natural CO₂ accumulations while about 3 MtCO₂ is captured from anthropogenic sources [6]. The SACROC project in Texas was the first large-scale commercial CO₂-EOR project in the world. It used anthropogenic CO₂ during the years 1972-1995. Similarly, Rangely Weber project uses anthropogenic CO₂ from a gas-processing plant in Wyoming. In Canada, CO₂-EOR project has been started at the Weyburn oil field. The project is expected to inject 23 MtCO₂ and extend the life of the oil field by 25 years [7,8]. CO₂-EOR projects are under way nowadays in the offshore North Sea reservoirs. Different projects are also currently under way in Trinidad, Turkey and Brazil [9].

Many CO₂ injection schemes have been suggested, including continuous gas injection (CGI) or water alternating gas (WAG) injection in miscible and immiscible injection modes. The displacement mechanisms range from oil swelling and viscosity reduction for immiscible CO₂ injection (below minimum miscibility pressure (MMP)) to completely miscible displacement in high-pressure applications (above MMP). Portion of injected gas returns with the produced oil. Therefore, it is usually re-injected into the reservoir to minimize operating costs [10].

The main objective of this study is to evaluate the performance of miscible CO₂ flooding at different conditions. To fulfill this objective extensive laboratory tests were conducted on 2 and 4 ft long sandstone cores using low and high salinity brine solutions as aqueous phase and three different oleic phases (n-Decane, Saudi-light and Saudi-medium crudes). Injection scheme ("CGI" versus "WAG"), WAG ratio, slug size, oil types, core orientation and core length were investigated. In addition, miscible WAG flooding as a secondary process was investigated and its efficiency was compared to the conventional tertiary miscible gas flooding.

CHAPTER 2

LITERATURE REVIEW

Enhanced Oil Recovery (EOR) essentially defined as the oil recovery by any method beyond the primary reservoir drive. These include pressure maintenance, water injection or other kind of techniques. Usually 5 to 40% of original oil in place is recovered by primary recovery methods [11]. Additional 10 to 20% of oil in place is produced by secondary methods such as water flooding [12]. Tertiary recovery methods, such as CO₂ flooding, have been practiced with incremental oil recovery of 7 to 23% of the original oil in place [13, 10], (see Figure 2.1). All the mentioned numbers depends on the properties of oil and the characteristics of the reservoir rocks. CO₂ could also be injected into depleted gas reservoirs to increase reservoir pressure and to enhance gas recovery although high percentage of original gas in place can be recovered primarily.

The appreciable decline in hydrocarbon reservoirs discovery and the increasing demand for oil and gas led the companies to explore the different EOR methods such as chemical, thermal and gas flooding. Carbon dioxide is an available gas and it becomes more attractive choice with the high environmental awareness of the harmful effects of GHG. Currently there are 75 CO₂-EOR projects world wide producing 194 million barrel per day most of which in united states [14].

When injected into the reservoir CO₂ interacts chemically and physically with the reservoir rock and the contained fluids, creating favorable conditions that improve oil recovery. These conditions include the following [14]:

1. Reducing the interfacial tension between oil and the reservoir rock that inhibit oil flow through the pores of the reservoir.
2. The expansion of oil volume and the subsequent reduction of its viscosity.
3. The development of complex phase changes in the oil that increases its fluidity.
4. The maintenance of favorable mobility characteristics for oil and CO₂ to improve the sweep efficiency.

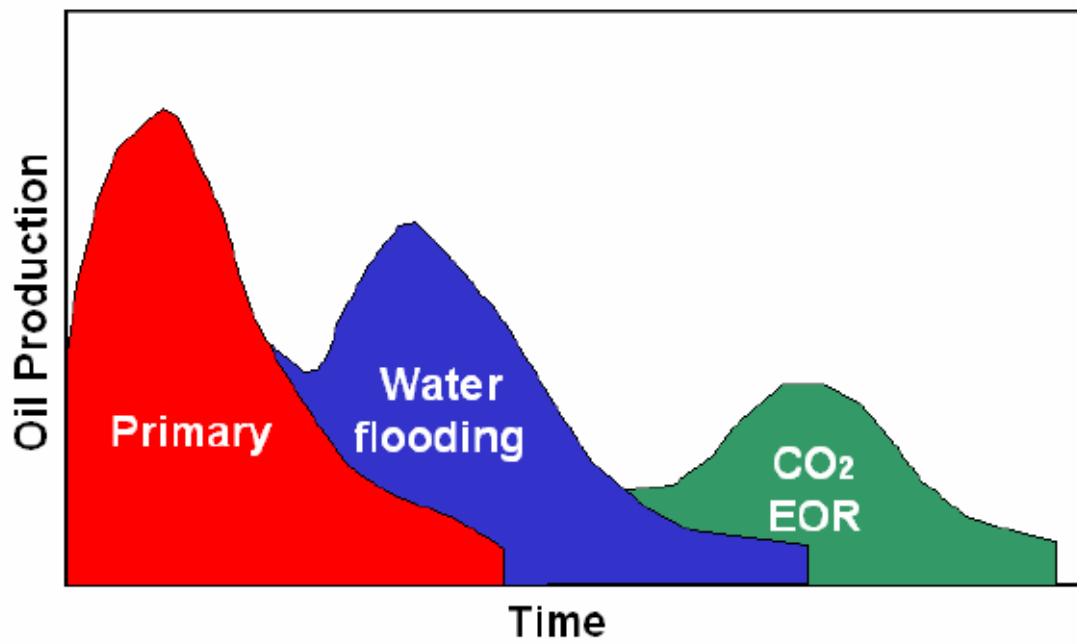


Figure 2.1: Oil recovery methods sequence in a typical oilfield [15].

Two processes have been performed for CO₂-EOR process. These are miscible and immiscible displacements. The applicability of each process depends on the reservoir conditions. CO₂ -EOR processes are also distinguished as CGI or WAG injection method. In WAG process, CO₂ is injected first to cause oil swelling and improve its fluidity. Another slug of water is then injected to displace the oil bank towards the production well. The concurrent flow of water and CO₂ results in the reduction of the mobility of each phase, reducing the occurrences of viscous fingering. In addition, the presence of water in the reservoir improves oil recovery, as it forms a fast diffusion path for CO₂ to reach oil trapped in the pores of the reservoir rock.

Another method of CO₂ injection is the immiscible gravity stable gas injection (GSGI) where CO₂ is injected in the crest at the gas zone, forcing the oil to move downwards towards the producing wells. WAG has an advantage over GSGI in that it can be performed on a small scale, while in general; GSGI is applied in the whole oilfield. Hence GSGI projects are likely to recover more oil and store larger CO₂ volumes [16, 17].

2.1 Miscible CO₂ Flooding

Under favorable crude oil composition and reservoir pressure and temperature, CO₂ can be miscible with oil, forming a single-phase liquid. As a result, the volume of oil swells and its viscosity and surface tension is reduced, improving the ability of the oil to flow and increasing oil recovery. CO₂ is not miscible with oil at first contact but miscibility develops dynamically through composition changes when the CO₂ gradually interacts with oil. This process is called multiple contact miscibility [16] (Figure 2.2).

The miscibility of CO₂-crude oil is strongly affected by MMP. The terminology (MMP) is the pressure at which CO₂ becomes fully miscible with oil. At that pressure, the density of CO₂ is similar to that of the crude oil [18, 19]. The value of MMP depends on the crude oil composition, the CO₂ gas purity and the reservoir pressure and temperature. Miscible CO₂ displacement can only be implemented when CO₂

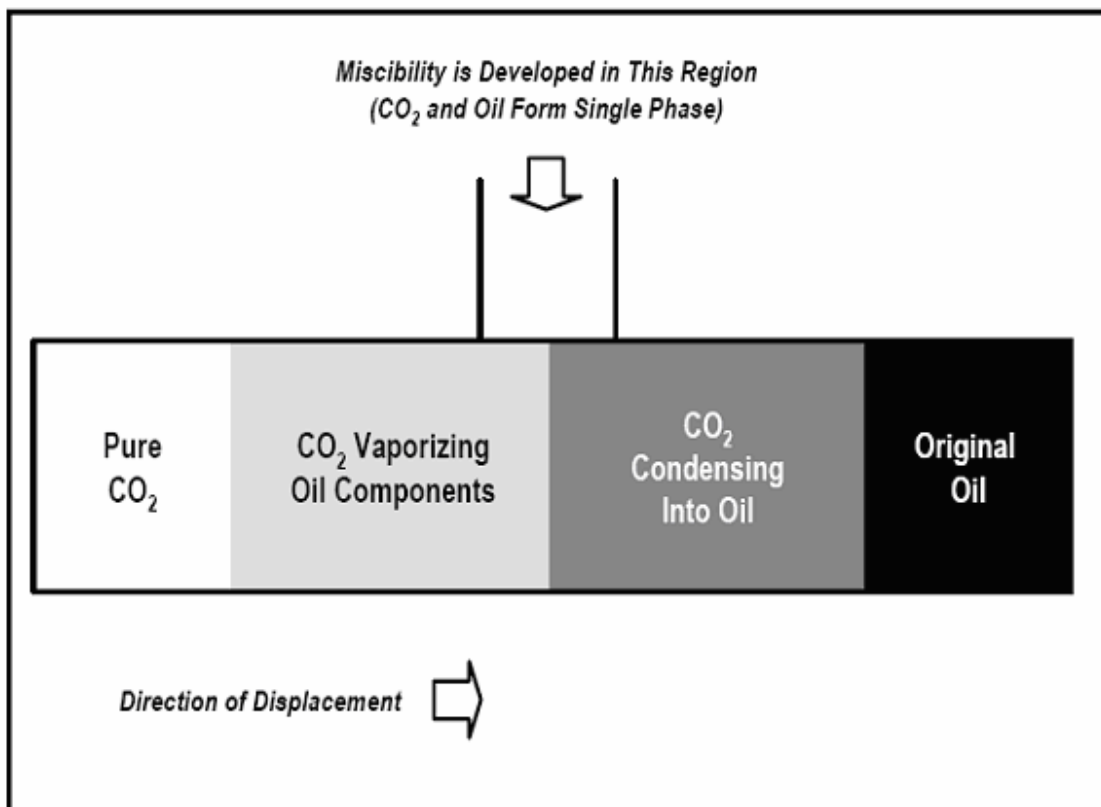


Figure 2.2: 1-D Schematic of The Dynamics CO₂ Miscible Process [16].

is injected at a pressure higher than the MMP, which must be lower than the reservoir pressure. MMP can nowadays be measured experimentally or predicted empirically and through thermodynamic modeling with a very good accuracy. A review of the current knowledge on the matter is presented in references [19, 20].

For miscible CO₂-EOR operations, oil reservoirs may need to meet specific criteria [21, 22, and 23]. Among these are reservoir depths, which must be more than 2500 ft to achieve miscibility because with shallower depths low miscibility pressure cannot be attained without fracturing the formation. Miscibility pressure usually increases with decreasing oil gravity. Therefore, Injection of miscible fluids is a good option of Low and medium viscosity oils (0.3 - 6 cp).

To prevent the occurrences of unstable flow and to reduce the amount of CO₂ needed for the process, CO₂ is typically injected into the reservoir alternately with water. WAG process was initially proposed to increase the sweep efficiency in gas flooding process. Generally WAG process is a combination of both traditional water flooding and gas injection techniques as shown in Figure 2.3. In this process, equal volumes of CO₂ and water slugs are injected in cycles at constant or different gas/water ratio, to improve sweep efficiencies of water flooding and miscible gas floods. The oil recovery improvement in WAG process is due to the mass transfer between the gas intermediate components and reservoir oil to develop miscible front. Expected increase in oil recovery by miscible WAG injection process presented in the literature are 10-15% in the Permian basin compared to 6 to 12% incremental recovery in some North Sea reservoirs using immiscible CO₂ flooding [16].

Data from 10 miscible displacement projects in the Permian basin indicate that the net injection of CO₂ into an oilfield is on average 164 m³ per barrel (bbl) of incremental oil. The evaluation of large number of US projects suggest that the average incremental recovery of oil lies in the range of 4-12% OOIP while the net volume of CO₂ injected is in the range of 10-45% of the OOIP. The highest oil recovery efficiencies are associated

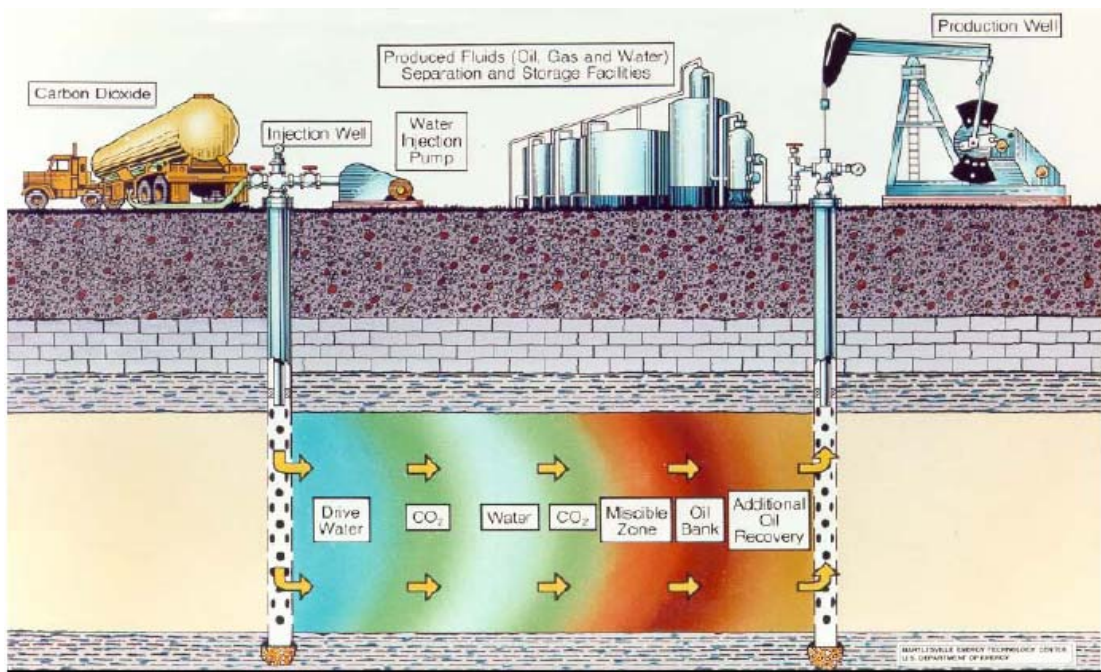


Figure 2.3: Schematic of a WAG miscible CO₂-EOR [16].

the tapered WAG injection process where the ratio of injected water to CO₂ changes with time, starting with larger CO₂ slugs that decrease in size with time [16].

General problems with miscible displacement that may cause failure can be summarized into the following:

- Insufficient reservoir geology and petrophysical information before starting a project.
- Reduction of reservoir pressure due to reduced injectivity caused by asphaltene deposition that may result in loss of miscibility and hence reduction of recovery.
- Failure of water pipelines and wells due to scale formation.
- Corrosion promoted by the carbonic acid formed by CO₂ dissolution in water.

2.1.1 Minimum Miscibility Pressure (MMP)

MMP is an important concept associated with the description of miscible gas injection processes. MMP is defined as the lowest pressure at which a crude oil and a solvent develop miscibility dynamically. At this pressure, the injected gas and the initial oil in place become multi contact miscible, and the displacement process becomes very efficient. If the displacement process is represented as a one dimensional, two-phase, dispersion-free flow, then at the MMP, the displacement is piston-like, and the oil recovery is 100% at 1 pore volume of gas injected.

The MMP is an important parameter in the design of a miscible gas injection project. The rationale behind the determination of MMP for a particular miscible gas injection project is that there is a trade off between achieving high oil recovery and reducing production costs. If the injection pressure is too low, the displacement would still be two-phase immiscible, and therefore the local displacement efficiency would be below the desired level. If the pressure is too high, although the displacement would become multi contact miscible, and the oil recovery would reach the desired level, the cost of pressurizing the injected gas would be larger than necessary. Hence an optimal pressure has to be found, and that pressure is MMP. A closely related concept is the minimum miscibility enrichment (MME). It is the enrichment level of a particular component or group of components in a

multi component injection gas for a given displacement pressure that causes the displacement to become multi contact miscible. Conceptually the MMP and MME are the same; they describe the same physical mechanism, one from the point of view of varying pressure to achieve miscibility, the other from the point of view of varying injection gas composition [24, 25].

Accurate determination of MMP or MME for a miscible gas injection process is of a considerable interest to the petroleum industry. Traditionally the MMP or MME is determined either experimentally or mathematically [24, 25].

2.1.1.1 Experimental Methods

There are several ways to measure MMP experimentally. The slim tube test is one of the most widely used techniques and is accepted as a standard mean to measure MMP in the petroleum industry. In a typical test, a slim tube made of stainless steel is packed with a porous material such as glass beads or sand. The tube is initially saturated with oil. Gas is injected at the inlet of the tube to displace oil at the desired test temperature and pressure. Effluent from the tube is collected and measured to obtain the recovery curve. Sometimes a visual cell is mounted downstream of the tube to allow visual inspection of the development of miscibility. The recovery data are plotted against the displacement pressures under which the tests are performed, and the recovery curve is used to infer the MMP. The criteria used by various investigators to determine the MMP from the oil recovery curve are different. A commonly used injection volume is 1.2 pore volumes. Fixed recovery levels defining MMP range from 90% to 95% [26, 27]. In addition, recovery values of 85% or 90% at breakthrough accompanied by 95% to 98% ultimate recovery have been used [28]. The bend in the recovery curve or point of maximum curvature is also used to define the minimum miscibility pressure [29, 30].

The point of maximum curvature occurs near the intersection of the extrapolated asymptotes of the low- and high-recovery regions. The pressure at which the recovery curve levels off is taken to be the MMP. Flock et al. [30] argued that the point of maximum curvature on the recovery curve is probably a better indication of miscibility. However, slim tube tests are expensive and time-consuming. The slim tube displacement test is often

referred to as the “industry standard” for determining MMP. Unfortunately; there is neither a standard design, nor a standard operating procedure, nor a standard set of criteria for determining MMP with a slim tube [24, 31]. The most widely schematic diagram of the slim tube test is shown in Figure 2.4.

The other experimental method for measuring MMP is the rising bubble experiment. In a typical rising bubble experiment, a glass tube is mounted in a high pressure sight gauge in a temperature controlled bath. The sight gauge is backlighted for visual observation and photography of rising gas bubbles in the oil. The glass tube is initially filled with oil. Injection gas bubbles are introduced to the glass tube and their shape and motion are observed and photographed for a range of pressures. An empirical pressure dependence of the behavior of the rising gas bubbles is established to infer the MMP. For simple condensing or vaporizing gas drives, Elsharkawy et al. [32] argued that MMPs measured by rising bubble experiments are consistent with MMPs obtained from slim tube test data.

Rising bubble experiments are appealing because they are much less time-consuming than slim tube tests. However, it is still not clear whether rising bubble experiments can be used to predict MMPs accurately for condensing/ vaporizing gas drives, which are far more common in crude oil displacements [33, 34].

The rising bubble apparatus [35] is shown schematically in Figure 2.5. The equipment consists of a high-pressure sight gauge with a rectangular flat tube with 1 mm fluid thickness and 5 mm width mounted in its centre, a bubble injector, three fluid storage vessels, a positive displacement pump, a temperature control unit, two pressure indicators, and a video recording system. In preparation for an experiment, the sight gauge and flat glass tube are filled with distilled water. The system is pressurized above the bubble point pressure of the reservoir fluid under investigation. The reservoir oil is then injected into the glass tube from the top to displace the water at a slow rate until the oil–water interface is slightly above the injector. Under this condition, the reservoir oil in the tube and water

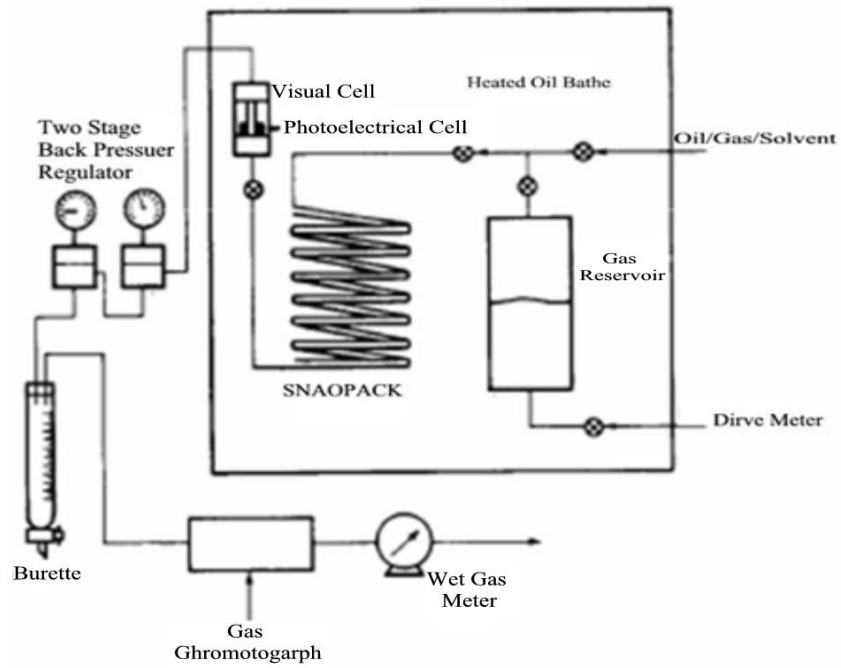


Figure 2.4: Slime tube apparatus [31].

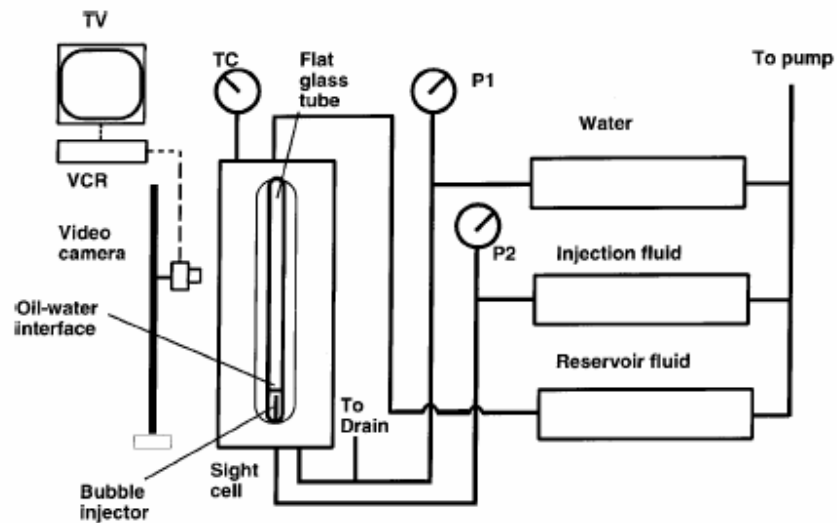


Figure 2.5: Schematic of the rising bubble apparatus [36].

around the tube are at the same pressure. A CO₂ bubble is launched into the water just beneath the oil–water interface. As the bubble rises through the oil–water interface and then the reservoir oil, its shape and motion are recorded. The movement of the bubble through the oil column mimics the forward contact between CO₂ and oil during the injection of a CO₂ slug through the reservoir. After one or two bubbles are injected into an oil sample, water is injected from the bottom to displace the used oil. Then, fresh oil is injected from the top to fill the glass tube for further rising bubble tests. For a gas–oil pair, rising bubble experiments are repeated over a range of pressures. The MMP is defined as the pressure at which the bubble and the oil showed multiple-contact miscibility [36].

2.1.1.2 Mathematical Determination of MMP

Various correlations reported in the literature (as shown in Table 2.1). These are related to a unique set of reservoir and fluid conditions; hence, using of such correlations can lead to an erroneous estimate of the MMP. The main factors affecting CO₂-oil MMP are reservoir temperature, oil composition, and purity of injected gas [29, 37, 38, 39, and 40]. The reservoir temperature has a big impact on CO₂-oil MMP; and as the temperature increases the MMP increases and vice versa. Rathmell et al. [41] reported that the presence of volatile components, like methane in crude oil leads to an increase in the CO₂-oil MMP, while the presence of intermediates C₂ to C₆ can reduce the CO₂-oil MMP. Metcalfe and Yarborough [42] argued that any CO₂-oil MMP correlation should take into consideration the presence of light and intermediates components in the crude oil. Alston et al. [38], in their experimental slim tube tests, proved that the oil recovery at gas breakthrough is decreased, and consequently CO₂-oil MMP is increased by increasing the ratio of volatiles to intermediates amounts in the crude oil composition. In addition, they stated that inclusion of molecular weight of C₅₊ enhances the correlation more than oil API gravity. Cronquist [43] used the temperature and molecular weight of C₅₊ as correlation parameters in addition to the volatile mole percentage of C₁ and N₂ in the crude oil.

Furthermore, the presence of non-CO₂ (e.g., C₁, H₂S, N₂, or intermediate hydrocarbons components (i.e. C₂, C₃, and C₄)) in the injected gas leads to a big impact on the CO₂-oil MMP, either raising or lowering it depending on the component type. In general, the-

Table 2.1: Commonly used CO₂-Oil MMP correlations

Reference	Correlation/model	Remarks
Pure CO₂-MMP Correlations		
Holm and Josendal [44]	A graphical correlation that is a function of reservoir temperature and C ₅₊ molecular weight of the crude oil.	-180 ≤ MW _{C₅₊} ≤ 240 -There are temperature and pressure limits for every molecular weight (that is, for MW _{C₅₊} = 240, temperature limit is from 32.2 to 82.2 °C, and pressure limit is from 9.65 MPa to 22 MPa).
	A graphical correlation that is a function of the amounts of C ₅ to C ₃₀ hydrocarbons present in C ₅₊ fraction, density of pure CO ₂ , and reservoir temperature.	-MMP is a linear function of the amounts of C ₅ -C ₃₀ hydrocarbon present in C ₅₊ fraction and the density of CO ₂ . • 53% ≤ (C ₅ -C ₃₀)/C ₅₊ ≤ 90%, • 6.9 MPa ≤ MMP ≤ 55 MPa, • 20 °C ≤ T _R ≤ 182 °C, If MMP < bubble point pressure (P _b), the P _b is taken as MMP.
Cronquist [43]	$MMP = 0.11027 \times (1.8T_R + 32)^y$, where $y = 0.744206 + 0.0011038 \times MW_{C_{5+}} + 0.0015279 * Vol$	The tested oil gravity ranged from 23.7 to 44 °API. -The tested T _R ranged from 21.67 to 120 °C. -The tested experimental MMP ranged from 7.4 to 34.5 MPa.
Lee, [45]	$MMP = 7.3942 \times 10^b$, where $b = 2.772 - \left(\frac{1519}{(492 + 1.8T_R)} \right)$	-Based on equating MMP with CO ₂ vapour pressure when T _R < CO ₂ critical temperature, while using the corresponding correlation when T _R ≥ CO ₂ critical temperature. -If MMP < P _b , the P _b is taken as MMP.
Yellig and Metcalfe [46]	$MMP = 12.6472 + 0.015531 \times (1.8T_R + 32) + 1.24192 \times 10^{-4} \times (1.8T_R + 32)^2 - 716.9427 / (1.8T_R + 32)$	Limitations: 35 °C ≤ T _R < 88.9 °C. -If MMP < P _b , the P _b is taken as MMP
Orr and Jensen [47]	$MMP = 0.101386 \times e^{\left(\frac{10.91 - \frac{2015}{255.372 + 0.5556 \times (1.8T_R + 32)}}{1} \right)}$	Based on extrapolated vapour pressure (EVP) method. Used to estimate the MMP for low-temperature reservoirs (T _R < 49 °C).
Glaso's [48]	When F _R > 18 mol%: $MMP = 5.58657 - 0.02347739 \times MW_{C_{7+}} + \left(1.1725 \times 10^{-11} \times MW_{C_{7+}}^{3.73} \times e^{786.8 \times MW_{C_{7+}}^{-1.058}} \right) \times (1.8T_R + 32)$	Considers the effect of intermediates (C ₂ -C ₆) only when F _R (C ₂ -C ₆) < 18 mol%.
	When F _R < 18 mol%: $MMP = 20.33 - 0.02347739 \times MW_{C_{7+}} + \left(1.1725 \times 10^{-11} \times MW_{C_{7+}}^{3.73} \times e^{786.8 \times MW_{C_{7+}}^{-1.058}} \right) \times (1.8T_R + 32) - 0.836 \times F_R$	

Table 2.1: Commonly used CO₂-Oil MMP correlations, continuation

Reference	Correlation/model	Remarks
Pure CO₂-MMP Correlations		
Alston et al. [38]	$MMP = 6.056 \times 10^{-6} \times (1.8T_R + 32)^{1.06} \times (MW_{C5+})^{1.78} \times \left(\frac{Vol}{Interm.} \right)^{0.136}$ <p>When $P_b < 0.345$ MPa</p> $MMP = 6.056 \times 10^{-6} \times (1.8T_R + 32)^{1.06} \times (MW_{C5+})^{1.78}$	If $MMP < P_b$, the P_b is taken as MMP.
Orr and silva [49]	$\rho_{MMP} = 0.524 \times F + 1.189, \text{ when } F < 1.467$ $\rho_{MMP} = 0.42, \text{ when } F > 1.467, \text{ where}$ $F = \sum_2^{37} K_i \times w_{iC2+}$ <p>and $\log(K_i) = 0.7611 - 0.04175 \times C_i$ and $w_{iC2+} = \frac{w_i}{\sum_2^{37} w_i}$</p>	<p>-MMP could be obtained at the reservoir temperature and ρ_{MMP}.</p> <p>-This correlation is used for pure and contaminated CO₂ injection.</p> <p>Limitations: This correlation does not take into consideration the presence of C₁ and all other non-hydrocarbons in the oil composition and can be used only when the carbon distribution from C₂ to C₃₇ is available.</p> <p>If $MMP < P_b$, the P_b is taken as MMP.</p>
Huang et al. (2003) neural network (ANN) model [50]	The pure CO ₂ -oil MMP is correlated with the molecular weight of C ₅₊ , reservoir temperature, and concentration of volatiles (methane) and intermediates (C ₂ -C ₄) in the oil.	When the temperature unit is changed from °F to °K, the model and the accuracy of the prediction is changed because the model will need to be retrained. Their training results that used to develop ANN model is that the average calibration error is 5.91% for °F and 6.48% for °K. While the output results of ANN model prediction is that the average relative errors are 12.08% for °F and 12.32% for °K.
Emera et al. (2004) [51]	$MMP = 5.0093 \times 10^{-5} \times (1.8T_R + 32)^{1.164} \times (MW_{C5+})^{1.2785} \times \left(\frac{Vol}{Interm.} \right)^{0.1073}$ <p>When $P_b < 0.345$ MPa</p> $MMP = 5.0093 \times 10^{-5} \times (1.8T_R + 32)^{1.164} \times (MW_{C5+})^{1.2785}$	<p>Based on Alston et al. [26] model, and adjusted their coefficients.</p> <p>Considered reservoir temperature, MW_{C5+}, and volatiles to intermediate ratio only.</p> <p>-If $MMP < P_b$, the P_b is taken as MMP</p>
Impure CO₂-MMP Correlations		
Alston et al. (1985) [38]	$\frac{MMP_{impure}}{MMP_{pure}} = \left(\frac{87.8}{1.8T_{CM} + 32} \right)^{\left(\frac{1.935 \times 87.8}{1.8T_{CM} + 32} \right)}, T_{CM} = \sum w_i \times T_{Ci}$	H ₂ S and C ₂ critical temperatures are modified to 51.67 °C

Table 2.1: Commonly used CO₂-Oil MMP correlations, continuation

Reference	Correlation/model	Remarks																
Impure CO₂-MMP Correlations																		
Sebastian et al. [29]	$\frac{MMP_{impure}}{MMP_{pure}} = 1.0 - 2.13 \times 10^{-2} (T_{CM} - 304.2) + 2.51 \times 10^{-4} \times (T_{CM} - 304.2)^2 - 2.35 \times 10^{-7} (T_{CM} - 304.2)^3,$ <p>wher : $T_{CM} = \sum x_i \times T_{Ci}$</p>	H ₂ S critical temperature is modified 325 °K (51.67 °C)																
Dong, [52]	$\frac{MMP_{impure}}{MMP_{pure}} = \left(\frac{T_{ac}}{304.2} \right)^4$ <p>Where,</p> $T_{ac} = \sum_{i=1}^n SF_i \times T_{Ci}$	<p>Dong (1999) used a factor (SF_i) representing the strength of species I in changing the apparent critical temperature of the impure CO₂ relative to the critical temperature of CO₂ (this factor is consistent with component K-values).</p> <p>The values of SF_i for different components are as follows:</p> <ul style="list-style-type: none"> -For H₂S, SF_i = 0.7 - For SO₂, SF_i = 0.5 -For C₁, SF_i = 2.5 - For O₂, SF_i = 5.0 -For N₂, SF_i = 7.5 - For CO₂, SF_i = 1.0 - For other non-CO₂ components, SF_i = 1.0 																
Emera et al. (2005) [40]	$\frac{P_{r,impure}}{P_{r,pure}} = 6.606 - 29.69 \times \left(\frac{1.8T_{CW} + 32}{1.8T_{C,CO_2} + 32} \right) + 109.5 \times \left(\frac{1.8T_{CW} + 32}{1.8T_{C,CO_2} + 32} \right)^2$ $- 213.363 \times \left(\frac{1.8T_{CW} + 32}{1.8T_{C,CO_2} + 32} \right)^3 + 208.366 \times \left(\frac{1.8T_{CW} + 32}{1.8T_{C,CO_2} + 32} \right)^4$ $- 98.46 \times \left(\frac{1.8T_{CW} + 32}{1.8T_{C,CO_2} + 32} \right)^5 + 18.009 \times \left(\frac{1.8T_{CW} + 32}{1.8T_{C,CO_2} + 32} \right)^6$ <p>where</p> $P_{r,impure} = \frac{MMP_{impure}}{P_{CW}}, P_{CW} = \sum_{i=1}^n w_i \times P_{Ci},$ $P_{r,pure} = \frac{MMP_{pure}}{P_{C,pure}}, \text{ and } T_{CW} = \sum_{i=1}^n MF_i w_i T_{Ci}$	<p>Based on the CO₂ critical properties (temperature and pressure), and the pure CO₂-oil MMP.</p> <p>Values of MF_i are as below:</p> <table border="1"> <thead> <tr> <th>Components</th> <th>MF_i</th> </tr> </thead> <tbody> <tr> <td>SO₂</td> <td>0.3</td> </tr> <tr> <td>H₂S</td> <td>0.59</td> </tr> <tr> <td>CO₂</td> <td>1.0</td> </tr> <tr> <td>C₂</td> <td>1.1</td> </tr> <tr> <td>C₁</td> <td>1.6</td> </tr> <tr> <td>N₂</td> <td>1.9</td> </tr> <tr> <td>All other injected gas Components</td> <td>1.0</td> </tr> </tbody> </table>	Components	MF _i	SO ₂	0.3	H ₂ S	0.59	CO ₂	1.0	C ₂	1.1	C ₁	1.6	N ₂	1.9	All other injected gas Components	1.0
Components	MF _i																	
SO ₂	0.3																	
H ₂ S	0.59																	
CO ₂	1.0																	
C ₂	1.1																	
C ₁	1.6																	
N ₂	1.9																	
All other injected gas Components	1.0																	

Table 2.1: Commonly used CO₂-Oil MMP correlations, continuation

Author	Correlation/model	Remarks
Impure CO₂-MMP Correlations		
Kovarik, [25]	$MMP_{impure} = 0.2814 \times (548 - (1.8T_{pc} + 492)) + MMP_{pure}$ <p>where</p> $T_{pc} = \sum_{i=1}^n w_i \times T_{ci} \text{ or } T_{pc} = \sum_{i=1}^n x_i \times T_{ci}$	<p>-The author stated that the weight average fraction correlated the data similar to the mole average fraction.</p> <p>-Limitation: Used only for C₁, as a non-CO₂ component, with less than 20- mole% ratios.</p>
Pure and Impure CO₂-MMP Correlations		
Eakin et al. (1988) [53]	<p>A graphical correlation that is a function of the reservoir temperature and molecular weight of C₅₊</p>	<p>Molecular weight of C₅₊ is modeled as a single alkane of equivalent molecular weight.</p> <p>Limitations:</p> <ul style="list-style-type: none"> ▪ 35 °C ≤ T_R ≤ 115 °C ▪ 156 ≤ MW_{C₅₊} ≤ 256 ▪ 7 MPa ≤ MMP ≤ 30 MPa
Johnson and Pollin [28]	$MMP - P_{Cinj} = \alpha_{inj} (T_R - T_{Cinj}) + I(\beta \times MW - M_{inj})^2$ <p>where:</p> $I = -11.73 + 6.313 \times 10^{-2} \times MW - 1.954 \times 10^{-4} \times MW^2 + 2.502 \times 10^{-7} \times MW^3 + (0.1362 + 1.138 \times 10^{-5} \times MW) \times \rho - 7.222 \times 10^{-5} \times \rho^2$ <p>where $\beta = 0.285$ and for pure CO₂, $\alpha_{inj} = 0.13$ MPa / °K</p> <p>-for N₂ impurity $\alpha_{inj} = 0.0722 \left(1.8 + \frac{10^3}{T_R - T_{Cinj}} \right)$</p> <p>-for C₁ impurity $\alpha_{inj} = 0.0722 \left(1.8 + \frac{10^2}{T_R - T_{Cinj}} \right)$</p>	<p>-Temperature range from 26.85 to 136.85 °C, used for less than 10% impurities in the injection gas,</p> <p>-Used for C₁ and/or N₂ impurities only.</p>
Yuan et al. [54]	$MMP = a_1 + a_2 MW_{C7+} + a_3 F_R + \left(a_4 + a_5 MW_{C7+} + a_6 \frac{F_R}{MW_{C7+}^2} \right) \times T_R$ $+ (a_7 + a_8 MW_{C7+} + a_9 MW_{C7+}^2 + a_{10} F_R) \times T_R^2$ $\frac{MMP_{impure}}{MMP_{pure}} = 1 + m \times (x_{CO_2} - 100)$	<p>a1 = -0.065996 a2 = -0.00015246 a3 = 0.0013807 a4 = 0.00062384 a5 = -0.00000067725 a6 = -0.027344 a7 = -0.0000026953 a8 = 0.000000017279 a9 = -0.000000000031436 a10 = -0.000000019566</p>

Table 2.1: Commonly used CO₂-Oil MMP correlations, continuation

Author	Correlation/model	Remarks					
Pure and Impure CO₂-MMP Correlations							
	$m = b_1 + b_2 MW_{C7+} + b_3 F_R + \left(b_4 + b_5 MW_{C7+} + b_6 \frac{F_R}{MW_{C7+}^2} \right) T_R + (b_7 + b_8 MW_{C7+} + b_9 MW_{C7+}^2 + b_{10} F_R) T_R^2$	b1 = -1463.4 b2 = 6.612 b3 = -44.979 b4 = 2.139 b5 = 0.11667 b6 = 8066.1 b7 = -0.12258 b8 = 0.0012883 b9 = -0.0000040152 b10 = -0.00092577 Used for injection CO ₂ streams contain up to 40 mole% of C1					
Shokir (2007) [20]	$MMP = -0.068616 \times z^3 + 0.31733 \times z^2 + 4.9804 \times z + 13.432$ <p>Where</p> $z = \sum_{n=1}^8 z_n, \text{ and}$ $z_n = A3_n x_n^3 + A2_n x_n^2 + A1_n x_n + A0_n$						
	n	types	x	A3	A2	A1	A0
	1	Oil components	T _R	+ 2.366E - 06	- 5.599E - 04	+ 7.534E - 02	- 2.918E + 00
	2		Vol., %	- 1.372E - 05	+ 1.364E - 03	- 7.917E - 03	- 3.123E - 01
	3		Interm., %	+ 3.555E - 05	- 2.785E - 03	+ 4.217E - 02	- 4.949E - 02
	4		MW _{C5+}	- 3.160E - 06	+ 1.986E - 03	- 3.975E - 01	+ 2.543E + 01
	5	Non-CO₂ components	C ₁ , %	+ 1.075E - 04	- 2.473E - 03	+ 7.095E - 02	- 2.965E - 01
	6		C ₂ -C ₄ , %	+ 6.945E - 06	- 7.919E - 05	- 4.492E - 02	+ 7.838E - 02
	7		N ₂ , %	0.0	+ 3.721E - 03	+ 1.979E - 01	+ 1.234E - 01
	8		H ₂ S, %	+ 3.907E - 06	- 2.772E - 04	- 8.901E - 03	+ 1.234E - 01

presence of H₂S, or intermediate hydrocarbon components in the injected gas decreases the CO₂-oil MMP, while the presence of C₁ or N₂ in the injected gas substantially increases the CO₂-oil MMP. N₂ from flue gas and C₁ from re-injected CO₂ are the large possible contaminants to CO₂ and recycled CO₂. The separation of such components from the injected gas is difficult and costly. The current trend is to use the flue gas stream as it is, if such impurities are below certain optimum level in the injected gas stream. Therefore, the developed model using the ACE algorithm, was designed to reach the optimal regression between the pure or impure CO₂-oil MMP and the reservoir temperature, mole percentage of oil components (volatiles (C₁ and N₂), intermediate components (C₂-C₄), and H₂S and CO₂), MWC₅₊, and mole percentage of the non-CO₂ components (C₁, N₂, H₂S, and C₂-C₄) in the injected CO₂.

2.2 Immiscible CO₂ Displacement Method

Immiscible CO₂ displacement process can enhance oil recovery especially in low pressure reservoirs or in case of recovering heavy oils. In immiscible displacement, CO₂ is injected to raise and maintain reservoir pressure. In addition, although not miscible with the reservoir fluids, CO₂ can partially dissolve in oil causing some swelling and viscosity reduction by a factor of 10. Immiscible CO₂ flooding is practiced in limited number of projects to raise reservoir pressure when rock permeability is too low or geologic conditions do not favor the use of usually practiced water flooding. In this process, CO₂ is typically injected in GSGI mode and to less extent in WAG mode. CO₂-GSGI is typically injected at slow rates at the reservoir crest to create an artificial gas cap, displacing oil downwards towards the production wells. This process may not be effective when applied after significant water flooding or when water present within the reservoir [16].

The immiscible displacement process has limited applications so far, due to the unfeasible economics. In immiscible project significant amounts of CO₂ are injected in the whole reservoir, limiting the opportunities for small-scale implementation to recover incremental oil at a very slow pace. However, immiscible displacement projects can store larger volumes of CO₂ than miscible ones making this process more attractive for CO₂ capture and storage.

Experience shows that the conditions that are favor in the immiscible displacement include [16]:

1. High vertical reservoir permeability.
2. Presence of substantial amount of oil to form a thick oil column.
3. Steep dipping and good lateral and vertical communication through the reservoir.
4. Absence of fractures that may reduce sweep efficiency.

An example of large immiscible displacement process is the Bati Raman oilfield, in southeast Turkey. The field contains heavy oil with very low gravity. CO₂ displacement oil recovery was 6.5% of OOIP compared to 1.5% using traditional oil recovery techniques [16]. A number of immiscible displacement pilot projects were initiated in the USA. However full commercial projects were not successful despite the promising results from the pilot studies [55]. Currently, one small-scale immiscible project is present in the USA, and 5 pilot projects in Trinidad [16, 55]. A number of immiscible displacement projects were also conducted in Hungary, using natural CO₂ reserve with overall CO₂ utilization of 380 m³/barrel of oil. Despite the small experience in immiscible displacement, it has been estimated that the utilization of CO₂ is within the range 280-400 m³ of CO₂ per barrel of incremental oil [16, 55]. It is expected that the process may yield approximately up to 20% of OOIP [24, 56].

2.3 Water Alternating Gas Injection (WAG) Process

Early Laboratory models conducted showed that simultaneous water/gas injection had sweep efficiency as high as 90%, compared to 60% for gas injection alone [57]. However, completion cost, operations complexity, and gravity segregation indicated that it is an impractical to minimize mobility. Therefore, a CO₂ slug followed by WAG has been adopted. The planned WAG ratios of 0.5:4 in frequencies of 0.1 to 2% PV slugs of each fluid cause water-saturation to increase during the water cycles and to decrease during the-gas cycle[58]. Claudle and Dyes [57] suggested simultaneous injection of water and gas to improve mobility control, however, the field reviews show that they are usually injected

separately [59]. There are important technical factors affecting WAG performance. These were identified as heterogeneity [60], wettability [18], reservoir fluids properties [61], miscibility conditions [60, 61], injection techniques [60, 61], WAG parameters [60, 61], physical dispersion [62], and flow geometry [60, 61] with most of the research work, conducted on either core flooding [57, 60] or numerical simulation [58, 61], sometimes alongside field trials.

A number of different WAG schemes are used to optimize recovery. Unocal patented a process called Hybrid WAG in which a large fraction of the pore volume of CO₂ is injected continuously, followed by the remaining fraction divided into 1:1 WAG ratios [63]. Shell developed a similar process called Denver Unit WAG (DUWAG14) by comparing continuous injection and WAG processes

The major design issues to be considered for WAG injection process are WAG ratio, injection rate, ultimate CO₂ slug size, reservoir characteristic and heterogeneity, rock and fluid characteristics, and injection pattern. In this thesis; I will concentrate on the literature discussing the parameters investigated in our laboratory so far such as WAG ratio and CO₂ slug size.

2.3.1 WAG Ratio

An optimum WAG ratio is a major design parameter that has a significant effect on operation and economics of a CO₂ flood. WAG ratio is defined as the ratio of injected water volume to CO₂ volume in each cycle. WAG ratios may be expressed in terms of barrels of water injected at reservoir conditions or in terms of the time of injection [64]. The WAG ratio is controlled by the gas availability as well as the reservoir rock wettability [65]. To maximize the net present value of CO₂ flood, WAG ratio should be increased gradually after the optimum gas production is reached [60]. The gradual increase of injected water (a decrease in the WAG ratio) results in increased mobility control and a constant produced gas profile. Laboratory studies [65] on WAG ratios showed that tertiary CO₂ floods have maximum recoveries at WAG ratio of about 1:1 in floods dominated by viscous fingering whereas continuous gas injection (0:1 WAG ratio) showed optimum recovery in floods dominated by gravity tonguing. Hence, continuous gas injection is

recommended for secondary as well as tertiary floods in water-wet rocks, whereas 1:1 WAG is recommended for partially oil-wet rocks. An analytical model indicated that the higher the WAG ratio, the lower the recovery but the better the mobility ratio. This suggests the importance of determining the optimum WAG ratio for WAG injection process [57, 60].

Simulation studies for Wasson Field, West Texas were carried out to investigate the important design issues for WAG process (WAG ratio and slug size). WAG injections at four different WAG ratios (1:1, 1:2, 2:1, and 4:1) were performed. The runs evaluated CO₂ slug sizes up to 100% hydrocarbon pore volume (HCPV). Results indicate that injecting a 100% HCPV slug of CO₂ with a 1:1 and 1:2 WAG ratio would yield the maximum incremental oil recovery [66] (See figure 2.6).

In practice all patterns may start at the same WAG ratio. Later, as the CO₂ production increases due to poor volumetric sweep efficiency, the WAG ratio is usually increased on a pattern-by-pattern basis starting with the highest GOR patterns [33].

2.3.2 Slug Size

Slug size refers to the cumulative CO₂ volume injected during a CO₂ flood. The slug volume is usually expressed as a percentage of rock pore volume or HCPV [64]. Optimum CO₂ slug size is critical in a proper design of miscible flooding [56]. Generally as more CO₂ volume injected, greater incremental oil is recovered. However, a large CO₂ slug size decreases the profitability of the project.

The optimum CO₂ slug size for a particular project depends on economical factors such as crude price, CO₂ cost, and the amount and timing of the incremental recovery. The economical optimization process is conducted by repeated simulation runs until optimum design parameters are achieved [67]. The ultimate CO₂ slug size can be determined after the start of project, when more information is known about future price of oil and production response of the reservoir. Total CO₂ slugs equal to about 20 to 50% HCPV has been used in different projects in U.S.A [68].

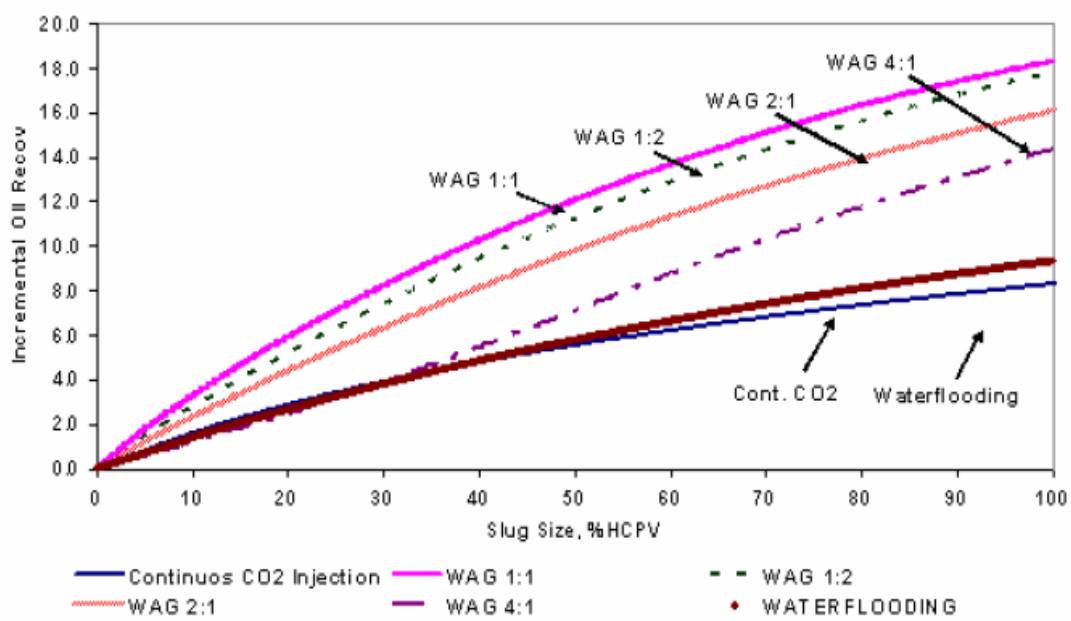


Figure 2.6: Comparison of different WAG ratios in terms of the incremental oil recovery as a function of the CO₂ slug size [66].

Numerical evaluation of single-slug, WAG, and Hybrid CO₂ injection processes for Dollarhide Devonian Unit, Andrews County, Texas was carried out [69]. Five slug sizes (8.8, 20, 30, 40, and 50% HCPV) were investigated to determine the optimal slug size to be used for the field application. It was found that the incremental oil recovery was increased and the ratio of incremental oil recovery to the amount of CO₂ injected decreased with increasing CO₂ slug size up to 30%. Above that the CO₂ flooding project is not feasible. A sensitivity study indicated that different WAG ratios from 0.5 to 2 did not affect oil recovery significantly as long as the total volume of CO₂ injected was identical and kept at 30% HCPV.

An experimental study conducted on long actual core using actual reservoir fluid samples of a carbonate oil reservoir indicated that an increasing CO₂ slug size enhances the oil recovery by miscible WAG flooding. However, the incremental oil recovery is not comparable to the increase in slug size and may be attributed to reduction in oil viscosity and increase of driving pressure [70].

CHAPTER 3

STATEMENT OF THE PROBLEM

The rising need for energy and the unimpressive oil recovery obtained through conventional methods, directed the industry attention to the EOR techniques for more oil recovery from the existing oilfields. CO₂ injection is considered one of the largest utilized enhanced oil recovery methods.

Sequestration of CO₂ and/or flue gas is not cheap; however, the injection of these gases into oil reservoirs to enhance oil production may offset some of the associated costs of doing this. With right reservoir conditions, injection of CO₂ into oil reservoirs can result in incremental oil recovery and permanent storage of CO₂ in geological formation. One of the most important factors in the selection of candidate reservoirs for gas injection is the minimum miscibility pressure at which miscible recovery takes place. Minimum MMP, as the name implies, is the minimum pressure at which the injection gas (CO₂ or hydrocarbon gas) can achieve multiple-contact miscibility with the reservoir oil. To increase the extent of the reservoir contacted by the displacing fluids, CO₂ is generally injected intermittently with water and this mode of injection, called WAG that is being widely practiced in the oil fields.

The major design issues to be considered for WAG injection process are WAG ratio, ultimate CO₂ slug size, fluid characteristics, and injection pattern. Therefore, the main objective of this study is to evaluate the performance of miscible CO₂ flooding at different conditions. To fulfill this objective extensive laboratory tests were conducted on 2 and 4 ft long sandstone cores using low and high salinity brine solutions as aqueous phase and three different oleic phases (n-Decane, Saudi light and medium crude oils). Injection scheme "CGI" versus "WAG", WAG ratio, slug size, oil types, core orientation and core length were investigated. In addition, miscible WAG flooding as a secondary process was investigated and its efficiency was compared to the conventional tertiary miscible gas flooding.

CHAPTER 4

EXPERIMENTAL APPARATUS AND PROCEDURE

This work is conducted to evaluate the efficiency of miscible CO₂ flooding. The aim is to investigate the effect of different parameters on gas flooding such as the mode of injection (WAG and CGI), WAG ratio, slug volume, oil composition and viscosity, brine composition, core orientation and core length. In addition secondary miscible WAG flooding at OOIP was investigated and compared to conventional miscible tertiary WAG flooding. This chapter will present the materials used, experimental set-up and the experimental procedure followed.

4.1 Rocks and Fluids

Core flooding experiments were conducted in Berea sandstone cores 2 inches in diameter, 2 and 4 ft long. Fresh core from a number of close permeability and porosity cores was used in each experiment. Pure Carbon Dioxide (99.5% purity) has been used as gaseous phase. n-Decane (99.9% purity), Saudi light and medium crude oils were used as the oleic phases. To investigate the effect of brine composition on miscible gas flooding, two types of saline solutions were used as aqueous phase. The first is identified as brine and it composed of 2.55% NaCl and 0.45% CaCl₂. The second is denoted as synthetic formation brine simulating Saudi formation brine solutions and composed of 5.89% NaCl, 2.24% CaCl₂ and 0.15% MgCl₂. Table 4.1 lists the physical properties of the used oleic and aqueous phases. In addition, Table 4.2 lists the chemical composition of the used Light and Medium Saudi crude oils.

MMP for the pure CO₂-oil binary systems were estimated using different empirical correlations at experimental temperature of 140°F. Table 4.3 lists the MMP values determined by Conquist [43], Lee [45], Yelling and Metcalfe [46], Orr and Jensen [47], Shokir [20], Yuan et al. [54], Glaso's [48], Emera and Sarma [40], and Alston et al. [38] correlations. The output of these correlations were validated with the experimental measurements of MMP conducted by Al-Shehri [71], and Orr and Jensen [47]. Al-shehri

Table 4.1: Physical properties of used n-Decane and aqueous solutions.

Fluid	Standard Conditions P= 14.7 psi, T= 60 °F	
	ρ (gm/cc)	μ (cp)
n-Decane	0.730	0.93
Brine (30 X 10 ³ ppm)	1.025	1.10
Formation Brine (82.8 X 10 ³ ppm)	1.062	1.30
Saudi light crude oil	0.853	9.0
Saudi medium crude oil	0.870	18.0

Table 4.2: Properties of the Saudi Crude Oils [71]

Component	Light	Medium
CO ₂ , mole %	0.16	0.06
H ₂ S, mole %	0	0
N ₂ , mole %	0	0
C ₁	0	0
C ₂ , mole %	0	0
C ₃ , mole %	0.08	0.19
n-C ₄ , mole %	0.22	0.36
i-C ₄ , mole %	2.28	2.09
n-C ₅ , mole %	1.9	1.8
i-C ₅ , mole %	4	3.34
C ₆ , mole %	6.26	5.56
C ₇₊ , mole %	85.1	86.6
MW _{C₅+}	228	230
MW _{C₇+}	249	269
API°	31.5	28

Table 4.3: Minimum miscibility pressure values of the binary oil-brine systems

Oil Type	T, °C	Exp. MMP, MPa	Shokir [20]		Yuan et al. [54]		Cronquist [43]		Emera and Sarma [40]		Glaso's [48]		Alston et al. [38]		Lee [45]		Yellig and Metcalfe [46]	
			MMP, MPa	Error, %	MMP, MPa	Error, %	MMP, MPa	Error, %	MMP, MPa	Error, %	MMP, MPa	Error, %	MMP, MPa	Error, %	MMP, MPa	Error, %	MMP, MPa	Error, %
Saudi Light Oil	60.0	---	14.90	---	19.96	---	15.11	---	14.43	---	15.61	---	17.93	---	12.86	---	12.13	---
	76.7	16.98	17.72	4.36	23.41	37.87	19.40	14.25	19.34	13.92	19.45	14.52	22.03	29.75	18.50	8.96	15.48	-8.83
	90.6	19.12	20.09	5.05	24.34	27.31	21.01	9.91	21.24	11.10	20.89	9.25	25.48	33.26	20.97	9.70	16.72	-12.5
Saudi Medium Oil	60.0	---	15.05	---	21.18	---	15.32	---	14.65	---	17.84	---	18.29	---	18.86	---	12.13	---
	76.7	18.53	17.92	-3.30	23.36	26.09	18.60	0.37	18.37	-0.84	21.05	13.62	22.47	21.29	16.97	-8.42	14.66	-20.9
	90.6	21.12	20.29	-3.94	24.43	15.69	21.33	0.99	21.56	2.10	23.73	12.35	25.99	23.07	20.97	-0.69	16.72	-20.8
N-Decane	71.1*	12.96	13.19	0.02	13.45	0.04	10.69	-0.18	10.70	-0.17	29.15	1.25	8.94	-0.31	15.52	0.20	13.83	0.07
	60.0	---	11.45		11.72		9.48		9.15		27.63		7.76		12.86		12.13	
ARE, %				0.44		21.40		5.07		5.22		10.20		21.41		1.95		-12.6
AARE, %				3.33		21.40		5.14		5.63		10.20		21.41		5.59		12.63

*Exp. MMP from Orr and Jensen [47].

* 1Psi = 6.9 X 10⁻³ MPa.

did his measurements on dead Saudi light and medium crud oils using slim tube at 76.7 and 90.6° C

To ensure good miscibility, the miscible floods were conducted at pressures slightly higher than the MMP value determined by experimental measurements and all empirical correlations mentioned above.

4.2 Experimental Setup

Flooding unit schematic was assembled after extensive literature search and consultations. Figure 4.1 is a schematic of the experimental flooding unit. It consists of two Hassler type core holders capable of housing a 2 ft and 4 ft long core samples both with 2 inches diameter core sample. Fluids were pumped using ISCO dual positive displacement syringe pump capable of displacing fluids at the desired injection rate or injection pressure. To save the pump from corrosive fluids, distilled water was pumped to the bottom of three two liters hastalloy floating piston transfer vessels filled with brine, oil and CO₂ gas to transfer these fluids to the core sample. Pressures at the inlet and outlet ends of the core holder were measured using 5000 psi pressure transducers. A network of high-pressure steel piping (1/8 inch) and a set of shutoff and three-way valves were used for fluid flow and flow direction control. The produced fluids were flown through digital backpressure regulator (DBPR) capable the pore pressure of the system up to 6000 psi. Gas coming out of the DBPR is vented through gas totalizer and water and oil are collected into a timely set fraction collector. The inlet, outlet and backpressure sensors were connected to data acquisition for timely based data logging. Several heating tapes with temperature controller were used to control the system components temperature.

4.3 Experimental Procedure

All experiments were started with fresh core sample evacuated and 100% saturated with brine under pressure. This was done by evacuating the core for few hours and displacing the core under vacuum at low rate with brine solution with the core outlet valve closed. The pumping continues and the pore pressure is raised to 1000 psi using the backpressure

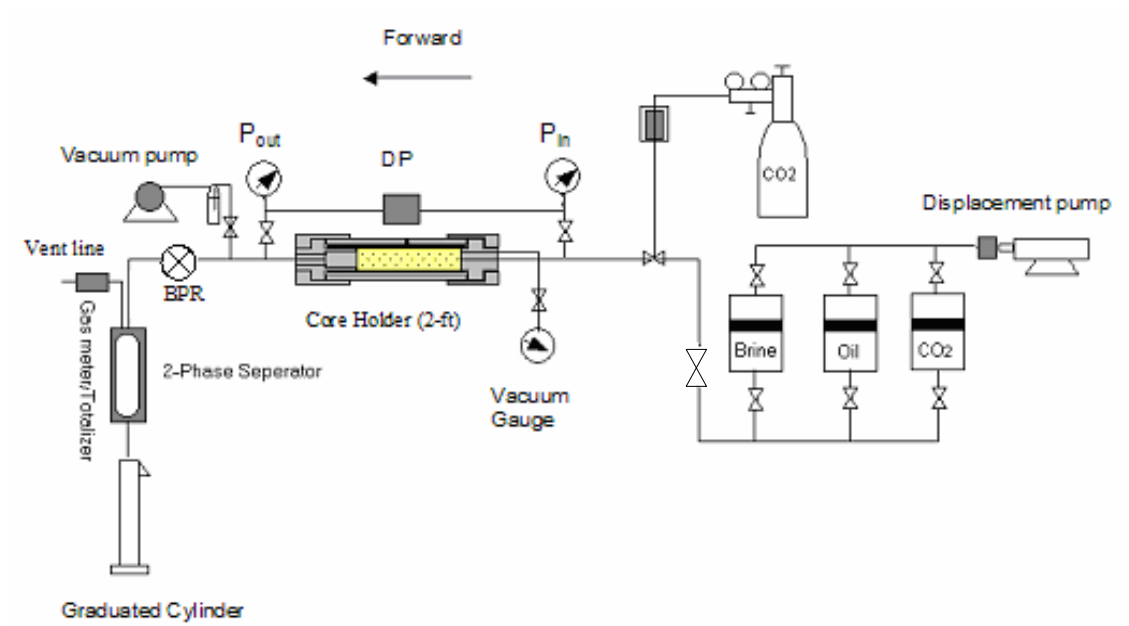


Figure 4.1: Schematic of the experimental set-up used in this study.

regulator. The pump is then shut down and the system was kept under pressure for a while. The inlet valve was then closed and the outlet valve was open and the compressed excessive brine is collected, weighed and subtracted with the lines dead volume from the brine volume pumped to determine the pore volume and hence the porosity.

The system temperature and pressure was raised to 60°C and to a net effective pressure ($P_{\text{confining}} - P_{\text{pore}}$) of about 600 psi and permeability was determined by pumping the fully saturated core at three different rates and measuring the pressure drop across the core ends. Darcy law was then used to calculate the absolute permeability.

The core sample was restored to reservoir saturation by injecting oleic phase from the oil transfer vessel into the brine-saturated core. This was done at 1.5 cc/min and continued until water production ceases. Connate water saturation (S_{wi}) was then determined using material balance and end effective oil permeability (K_o) was measured using Darcy law. The core is now at its initial water saturation, and the core is left for wettability restoration and oil-water distributions refinement at the pore level. Water flooding was then started at 1.5 cc/min to residual oil saturation (S_{or}). The effluents volumes and pressure drop were measured continuously and recorded as a function of time. This was continued until no more oil is produced. Effective water permeability (K_w) was calculated using Darcy law and post secondary water flooding residual oil saturation (S_{or}) was determined through material balance.

At the end of the imbibition process (Berea is generally considered water-wet rock), significant residual oil remains in the pore space. Therefore, tertiary CO₂ flooding was carried out subsequent to the secondary water flooding process. This was done in either CGI or WAG injection schemes. The CGI was conducted by flooding the core with CO₂ at constant pressure. The injection pressure is chosen to be above the miscibility pressure of the fluid pair used providing a flow rate range of 1.5-3 cc/min to ensure stability of the flood. The brine and oil produced were collected in graduated glass tubes mounted in a fraction collector while gas produced at the outlet end was vented through gas totalizer.

Water alternating gas injection is conducted by flooding CO₂ and water alternately with different WAG ratios at different slug sizes for every WAG ratio. Similar pressure in both the brine and gas transfer vessels was maintained to prevent instabilities and early breakthrough during the flood. Again, the brine and oil volumes produced were collected in graduated glass tubes mounted in timely set fraction collector while gas produced was vented through gas totalizer. The scaling rule of Leas and Rappaport [72] was used to ensure stable oil, water and gas flooding.

CHAPTER 5

RESULTS AND DISCUSSIONS

Fifteen experiments were conducted to investigate the effect of different parameters on oil recovery of miscible CO₂ flooding. These parameters included the injection mode (CGI and WAG), oil type, brine composition, WAG ratio, slug size, core orientation and core length. WAG as a secondary process was investigated and compared to the conventional tertiary WAG gas flooding. Table 5.1 lists the measured physical rock properties of porosity and permeability, water flooding recovery factor, post secondary flooding end-point saturations and end point effective permeability values for the experimental runs conducted.

As mentioned previously, the core preparation consisted of different sequential steps, including core saturation with aqueous phase, oil flooding to initial water saturation at the flood out, and water flooding to residual oil saturation at flood out. The water flooding process was applied to simulate the secondary oil recovery process. Subsequent to the secondary flooding process, the core samples were subjected to miscible CO₂ flooding to recover an incremental portion of the residual oil in place (ROIP). Figure 5.1 shows the recovery curve of the water flooding process performed in run 15 listed in Table 5.1. This curve is a typical representation of all the water flooding recovery curves obtained in all conducted experiments. This chapter outlines the results for the miscible flooding experimental work

Miscibility controls the microscopic displacement efficiency by affecting the capillary number due to lowering of the interfacial tension. At the end of water flooding stage, the core samples were miscibly flooded with CO₂. Table 5.2 summarizes the experiments conditions and the output of all conducted miscible gas flooding runs listing the oil recovery (RF) as a percentage of residual oil in place (% ROIP), oil recovery as a percentage of original oil in place (% OOIP), and the maximum tertiary recovery factor (TRF) and the corresponding pore volume of gas injection. The obtained CO₂ flooding results and the effect of different investigated parameters are discussed extensively in the following sections.

Table 5.1: Petrophysical properties of water flooded rock samples.

Exp. No.	WAG Ratio	Slug Size	core Length, ft	Core Orientation	Aqueous Phase	Oleic Phase	Φ , %	K, md	K_o , md	S_{wi} @ flood out, %	K_w , md	S_{or} @ flood out, %	RF after Water Flooding, %OOIP
1	1:1	0.2	2	Horizontal	Brine	n-Decane	22.26	275.47	122.15	46	227.44	41.1	24.06
2	1:2	0.2	2	Horizontal	Brine	n-Decane	21.52	283.46	134.36	46.6	39.04	42.1	21.2
3	1:1	0.4	2	Horizontal	Brine	n-Decane	19.9	295.98	155.2	43.84	39.42	41.09	26.84
4	1:1	0.6	2	Horizontal	Brine	n-Decane	20.64	248.42	165.03	42.03	158.85	42.34	26.97
5	1:2	0.4	2	Horizontal	Brine	n-Decane	19.8	247.43	159.39	46	39.81	39.9	26.24
6	2:1	0.4	2	Horizontal	Brine	n-Decane	19.74	293.65	127.18	47	45.42	42.5	20.17
7	CGI		2	Horizontal	Brine	n-Decane	19.79	287.68	140.02	45	37.41	39.7	28.35
8	1:2	0.2	2	Horizontal	Formation brine	n-Decane	19.61	393.61	116.23	44.9	44.9	41.8	24.18
9	1:2, 0.2PV @ Secondary flooding		2	Horizontal	Brine	n-Decane	19.89	245.46	143.54	47	-	-	-
10	1:1	0.2	2	Horizontal	Formation brine	Light Crude Oil	19.74	281.89	55.79	34.2	27.09	45.23	31.3
11	1:2	0.2	2	Horizontal	Formation brine	Light Crude Oil	19.69	281.89	90.66	37	35.71	43.03	31.72
12	1:2	0.2	2	Vertical	Formation brine	Light Crude Oil	19.81	281.89	50.37	32.9	24.18	50.02	25.48
13	1:2	0.2	4	Horizontal	Formation brine	Light Crude Oil	19.76	383.17	136.04	35.4	30.9	39.21	39.34
14	CGI		4	Horizontal	Formation brine	Light Crude Oil	19.57	347.99	78.25	34.8	30.9	41.39	36.48
15	1:2	0.2	2	Horizontal	Formation brine	Medium Crude Oil	19.48	316.8	22.15	31.8	17.22	46.98	36.94

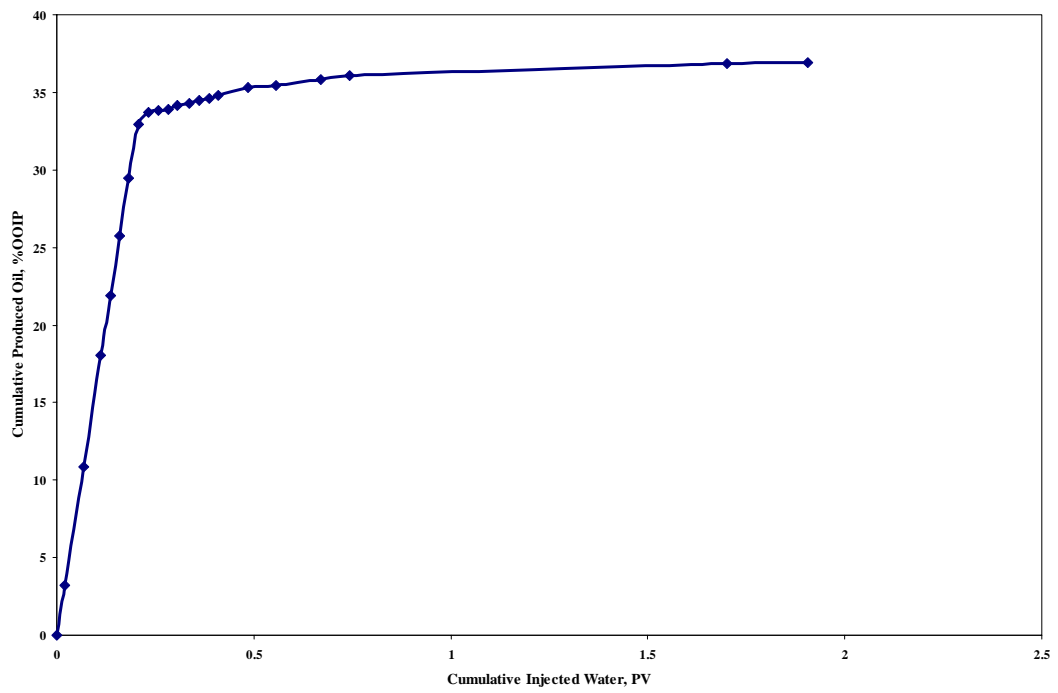


Figure 5.1: Cumulative oil recovery versus cumulative water volume injected during the water flood process on run 15.

Table 5.2: Summary of conducted miscible gas flooding experimental runs

Exp. No.	WAG Ratio	Slug Size	core Length, ft	Core Orientation	Aqueous Phase	Oleic Phase	Exp. Pressure, Psi	Cum. Gas & Water Inj., PV	Cum. Gas Inj., PV	TRF, %/PV	RF, %ROIP	RF, %OOIP	Utilization Factor, Mscf/Bbl
1	1:1	0.2	2	Horizontal	Brine	n-Decane	2145	0.9	0.5	23	18	14	44.14
								2.2	1.2	45.1	54.12	41.1	10
								3.4	1.8	30.1	54.18	41.14	15
2	1:2	0.2	2	Horizontal	Brine	n-Decane	2370	0.7	0.5	34.9	17.5	13.8	14.4
								1	0.8	65.6	52.6	41.45	7.66
								2.4	1.8	43.2	77.85	61.35	11.62
3	1:1	0.4	2	Horizontal	Brine	n-Decane	2333	0.9	0.5	19.23	9.62	7.04	26.3
								1.7	0.9	56.09	50.5	36.94	9
								3.4	1.8	40.73	73.32	53.64	12.4
4	1:1	0.6	2	Horizontal	Brine	n-Decane	2110	0.5	0.5	0	0	0	--
								3.7	1.9	31.7	59.6	43.53	12.5
								3	1.8	30.4	54.7	39.94	13.98
5	1:2	0.4	2	Horizontal	Brine	n-Decane	2325	0.5	0.5	0	0	0	--
								1.5	1.1	47.9	52.4	38.66	10.82
								2.6	1.8	43.2	77.31	57.02	12.1
6	2:1	0.4	2	Horizontal	Brine	n-Decane	2325	1.3	0.5	0	0	0	--
								3.7	1.3	47	61.1	48.77	10.48
								5	1.8	42.5	76.5	61.07	11.44
7	CGI		2	Horizontal	Brine	n-Decane	2325	0.5	0.5	53.7	26.4	18.92	9.87
								0.7	0.7	71.7	50.2	35.97	7.26
								1.8	1.8	48.45	87.2	62.48	10.74
8	1:2	0.2	2	Horizontal	Formation brine	n-Decane	2250	0.7	0.5	105.8	52.9	40.11	4.19
								0.7	0.5	105.8	52.9	40.11	4.19
								2.6	1.8	42.74	76.92	58.32	14.55
9	1:2, 0.2PV @ Secondary flooding		2	Horizontal	Brine	n-Decane	2240	0.7	0.5	14.6	7.3	7.3	25.15
								2.15	1.55	48.7	75	75	9.08
								2.6	1.8	45.8	82.4	82.4	8

Table 5.2: Summary of conducted miscible gas flooding experimental runs, continuation

Exp. No.	WAG Ratio	Slug Size	core Length, ft	Core Orientation	Aqueous Phase	Oleic Phase	Exp. Pres., Psi	Cum. Gas & Water Inj. PV	Cum. Gas Inj. PV	TRF, %/PV	RF, %ROIP	RF, %OOIP	Utilization Factor, Mscf/Bbl
10	1:1	0.2	2	Horizontal	Formation brine	Light Crude Oil	2800	0.9	0.5	55.25	27.5	18.89	11.2
								0.87	0.47	55.75	26.1	17.93	11.1
								3.4	1.8	26.49	47.7	32.77	23.33
11	1:2	0.2	2	Horizontal	Formation brine	Light Crude Oil	2800	0.7	0.5	74	37	25.26	11.14
								0.8	0.6	81.3	48.8	33.32	10.62
								2.6	1.8	34	61.2	41.79	25.8
12	1:2	0.2	2	Vertical	Formation brine	Light Crude Oil	2800	0.7	0.5	73	36.5	27.2	9.04
								0.7	0.5	73	36.5	27.2	9.04
								2.6	1.8	26.8	47.3	35.25	30.63
13	1:2	0.2	4	Horizontal	Formation brine	Light Crude Oil	2700	0.7	0.5	101	50.5	30.63	6.8
								0.7	0.5	101	50.5	30.63	6.8
								2.6	1.8	34.3	61.7	37.43	20.5
14	CGI		4	Horizontal	Formation brine	Light Crude Oil	2700	0.5	0.5	87.9	44	27.95	7.4
								0.4	0.4	89.9	36	22.87	7.2
								1.8	1.8	27	46.7	29.63	24.8
15	1:2	0.2	2	Horizontal	Formation brine	Medium Crude Oil	3400	0.7	0.5	67.6	33.8	23.28	9.61
								0.7	0.5	67.6	33.8	23.28	9.61
								2.6	1.8	27	48.6	33.48	23.7

5.1 Effect of Slug Size

The selection of the optimum slug size for CO₂ flooding is a crucial economical factor. Generally, the higher the amount of gas injected, the greater the incremental oil recovery. On the other hand, a large gas slug size diminishes the financial return of the project. To investigate the effect of this parameter, n-Decane-brine fluid pair was used in three experiments conducted at 1:1 WAG ratio at different slug sizes of 0.2, 0.4 and 0.6 PV. Figure 5.2 presents the obtained recovery curves indicating an ultimate oil recovery factor (RF) of 59.0, 78.1, and 67.5 % ROIP for the 0.2, 0.4, 0.6 PV slug sizes experiments respectively. With the initiation of the first slug of CO₂ into the core, gas saturates and displaces the resident water and simultaneously diffuses and dissolves in and swells the residual oil. That results in no oil recovery and only water production in that slug of gas injection for these runs and all those experiments to be discussed in the following sections. Appreciable delay on approaching reasonable ultimate oil recovery was also noticed when increasing slug size especially for the case of 0.6 PV slug size.

Due to the unequal quantities of cumulative gas injection for the three runs, recoveries are normalized in order to accurately examine the optimum slug size. Therefore, a term named tertiary recovery factor (TRF) was used and it is defined as follows;

$$\text{TRF} = [(\text{Oil produced, cc}) / (\text{ROIP, cc}) * 100] / [\text{Injected CO}_2, \text{PV}] \dots \dots \dots (5.1)$$

Where,

ROIP is the residual oil left in place at the end of the secondary water flooding process. Figure 5.3 shows TRF versus cumulative pore volume of gas injection for the runs conducted at the three different slug sizes. Maximum TRF obtained for 0.2 PV slug size was 45.1 after 1.2 PV of gas injection. The resulted maximum TRF for 0.4 PV slug size shows a higher value of 56.0 at a total gas injection of 0.9 PV. Both slug sizes show an exponential decline in TRF after reaching the peak value.

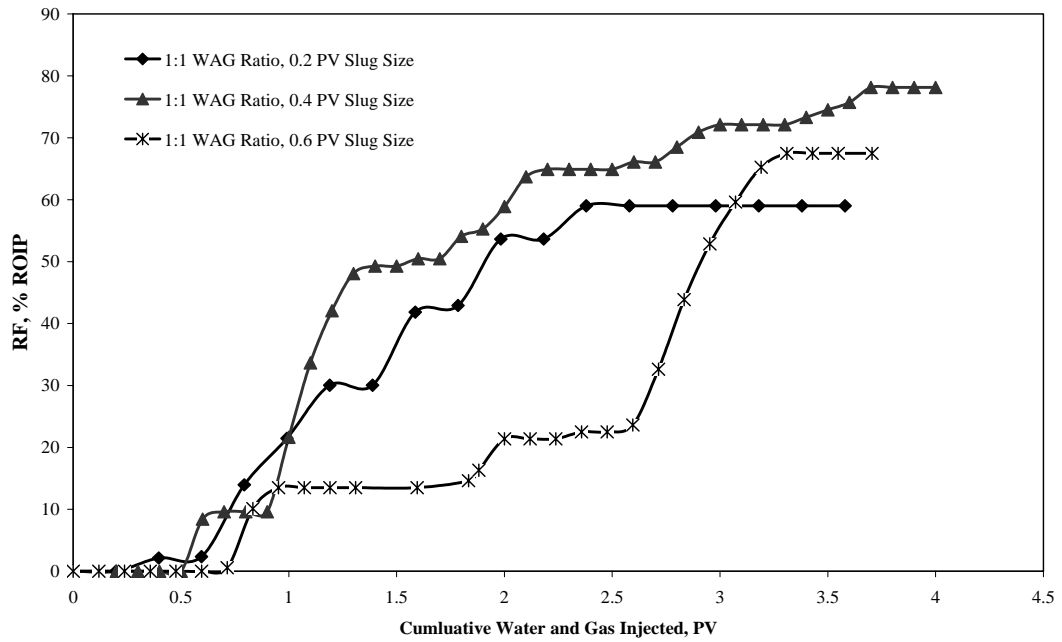


Figure 5.2: Effect of slug size on recovery factor of 1:1 miscible WAG displacement experiments using n-Decane-brine fluid pair.

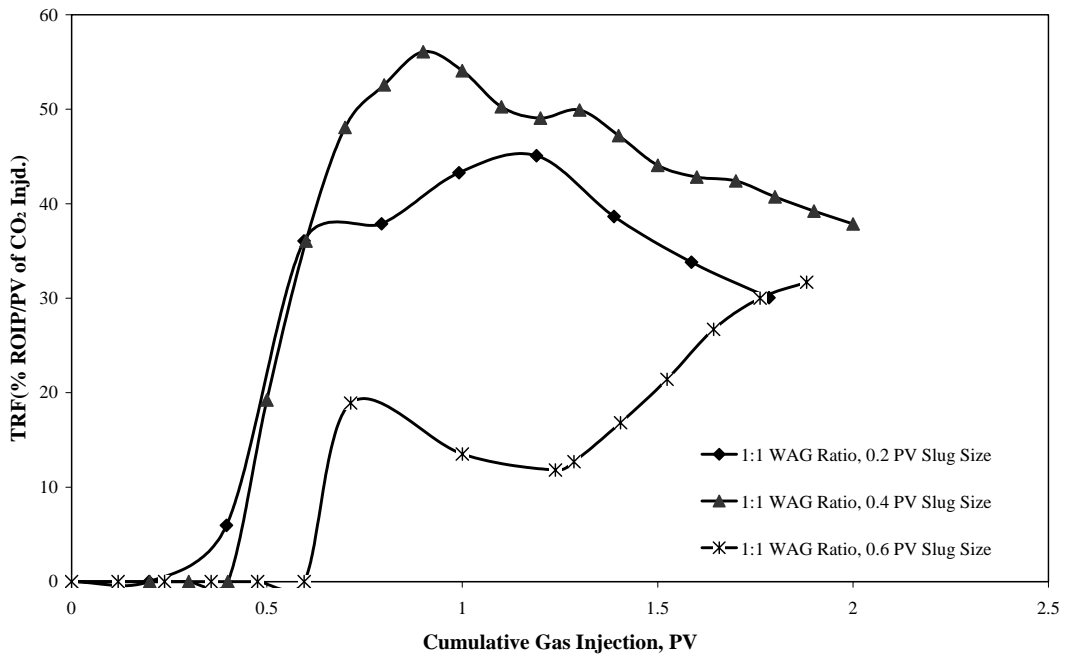


Figure 5.3: Effect of slug size on tertiary recovery factor of miscible 1:1 WAG displacement experiments using n-Decane-brine fluid pair.

The obtained TRF curve at 0.6 slug size shows an early TRF peak of 19.0 obtained after a cumulative gas injection of 0.7 PV. This was followed by a drop in TRF then a gradual increase to a maximum TRF of 31.7 after a cumulative gas injection of 1.9 PV. From economical point of view, unless this incremental oil recovery caused by the additional volume of gas injection is feasible, the first peak is considered to represent the optimum tertiary recovery factor.

From the recovery factor and TRF curves of the three experiments, 1:1 WAG at 0.4 PV slug size seems to be the best flooding scenario among this set of experiments. This output agrees well with the previous work conducted by Huang and Holm [58] who indicated that additional oil recovery would become less and less as CO₂ slug size increases higher than 0.4 PV. Any additional gas injection will sweep little additional oil since it will, due to gravity segregation, follow the low resistance path at the top of the porous media filled by gas that had already swept the oil in that part by previous slugs [73] It is worth noting that 0.2 PV slug size experiment was stopped early with a clear increasing trend, therefore the ultimate recovery recorded is less than what is expected. Therefore, based on the experimental findings and the confirmation of other researchers, further increase in slug size above 0.4 PV is not feasible. Early during the gas injection process, 0.2 PV slug size gives similar to slightly higher TRF values. This may direct us to suggest injecting at 0.2 PV slug size until the peak TRF and switch to 0.4 PV to approach higher ultimate recovery with least volume of gas injection.

Further experiments were conducted using n-Decane-brine fluid pair to study the effect of slug size on oil recovery for 1:2 WAG ratio at two slug sizes of 0.2 and 0.4 PV. Figure 5.4 presents the oil recovery factor versus the cumulative pore volume of water and gas injected. The figure indicates an ultimate oil recovery of 80.0 and 86.0 % ROIP for the 0.2 and 0.4 PV slug sizes respectively. This was accomplished after a cumulative alternating water and gas injection up to 3.5 PV. Again, recoveries are normalized to evaluate the performance of the two runs and TRF curves are plotted in Figure 5.5 as a function of cumulative pore volumes of gas injection.

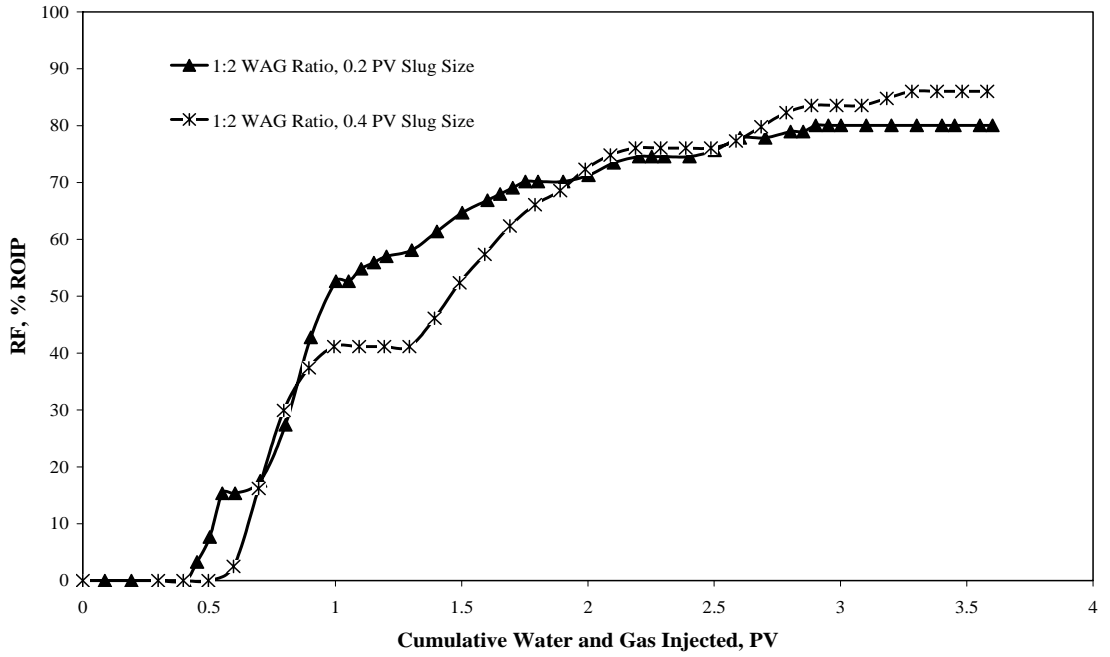


Figure 5.4: Effect of slug size on recovery factor of miscible 1:2 WAG displacement experiments using n-Decane-brine fluid pair.

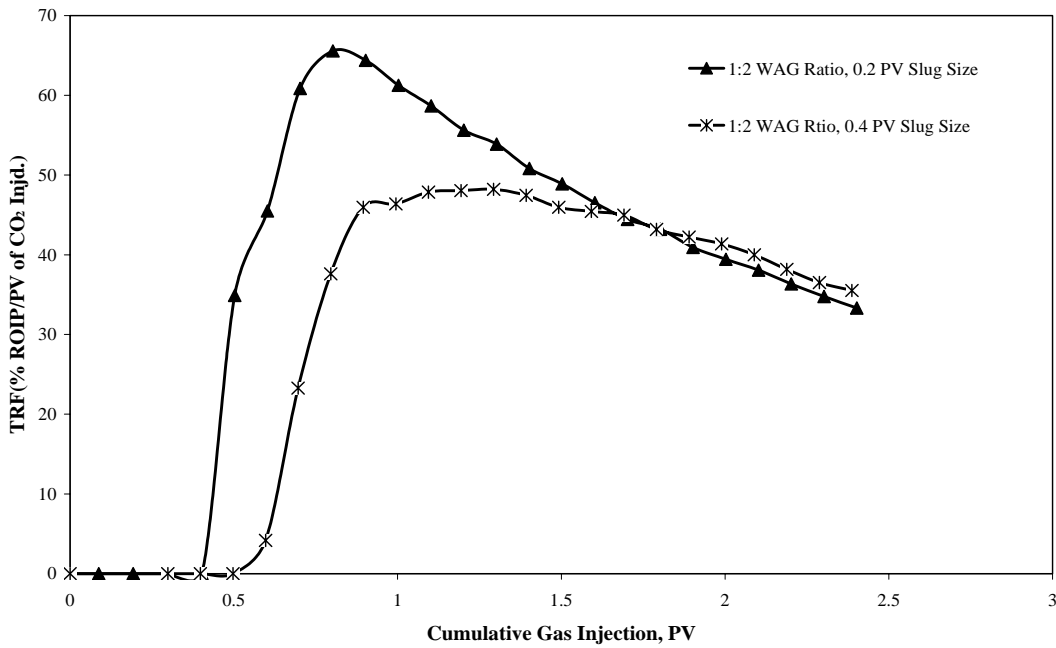


Figure 5.5: Effect of slug size on tertiary recovery factor of miscible 1:2 WAG displacement experiments using n-Decane-brine fluid pair.

The figure indicates a maximum TRF of 65.6 after a cumulative gas injection of 0.8 PV for 0.2 PV slug size compared to a TRF of 47.9 after gas injection of 1.1 PV for the 0.4 PV slug size. It is interesting to note that what seems to be showing a better performance based on recovery factor indicate a lower performance based on TRF. This is due to the increasing volume of gas injection with the increase in slug size. Further injection of gas beyond the peak TRF resulted in additional oil recovery for both slug sizes, but a reduction in TRF due to the reduction of oil production and the increases of gas injection needed to mobilize that oil.

Comparing the two determined best slug sizes of the 1:1 and 1:2 WAG ratios, it is obvious that the volume of water injected in both cases was the same but the volume of gas injection was doubled for the 1:2 WAG compared to that of 1:1 WAG ratio. Therefore, further experiments were conducted to investigate the effect of WAG ratio on recovery performance.

5.2 Effect of WAG Ratio

The WAG injection process is performed to improve the macroscopic and microscopic sweep efficiency. WAG flooding must be carefully evaluated, since water saturation is increased to the extent of produced oil. The increased water saturation might have a negative impact on oil displacement, since part of oil may become inaccessible to CO₂ [58]. Therefore, it was decided to investigate the effect of WAG ratio on oil recovery in order to determine the optimum ratio. Experiments conducted using n-Decane-brine fluid pair was compared at different 1:1, 1:2 and 2:1 WAG ratios. All were carried out at 0.4 PV slug size. In the 1:2 WAG ratio experiment, the volume of gas injected is two times that injected at 1:1 WAG ratio, while the volume of injected water is the same. On the other hand, the water volume was two times greater than the gas for the 2:1 WAG case compared to 1:1 or 1:2. Figure 5.6 shows the oil recovery curves and it indicates that 1:1 and 2:1 WAG ratios produced a close ultimate recovery of 78.1 % and 79.8 % ROIP respectively compared to higher recovery of 86.0 % ROIP for 1:2 WAG ratio case. Ultimate recovery obtained using 2:1 WAG ratio was made after large cumulative water and gas injection, which makes it economically non-feasible compared to the other two WAG ratios.

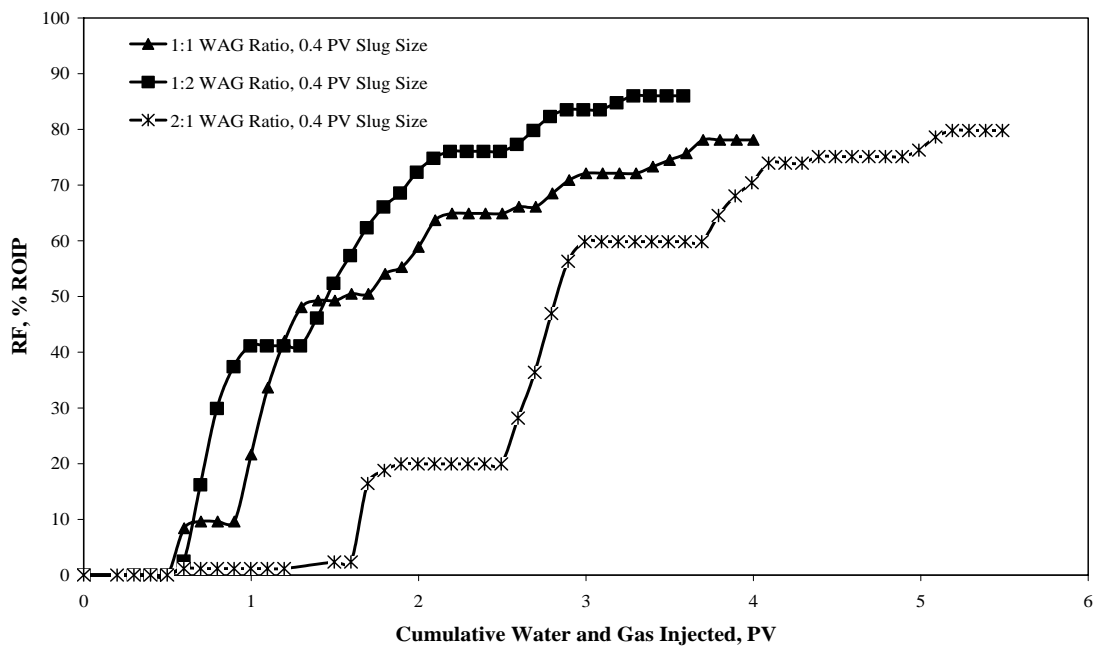


Figure 5.6: Effect of miscible WAG ratio on recovery factor for 0.4 PV slug size displacement experiments using n-Decane-brine fluid pair.

Mohanty [74] indicated that oil recovery is obtained faster with decreased WAG ratio. More solvent is injected for lower WAG ratio at any given time and miscible solvent is more effective than water in oil recovery. This explains the advantage of 1:2 WAG ratio over the other two.

Figure 5.7 presents a comparison of the TRF curves for the three runs conducted at different WAG ratios. The figure shows that 1:1 WAG ratio yielded the highest peak TRF compared to the other two with peak TRF value of 56.1 after 0.9 PV of gas injection. 1:2 and 2:1 WAG ratios show close peak TRF values of 47.9 after 1.1 PV and 47 after 1.3 PV of gas injection respectively. Based on recovery 1:2 seems to be the optimum WAG ratio but based on TRF 1:1 seems to give better performance due to earlier recovery with the least amount of gas injected. Therefore, the decision on the best WAG ratio should be decided based on the economics taking into consideration both the incremental oil recovery and the cost and the availability of CO₂.

For more investigation on the effect of WAG ratio on oil recovery, Saudi light crude-synthetic formation brine fluid pair was used in two runs at different WAG ratios of 1:1 and 1:2, both at the same slug size of 0.2 PV. Figure 5.8 presents the recovery curves for the two runs indicating oil recovery factor of 51 % ROIP for 1:1 WAG ratio compared to 63 % ROIP for the 1:2 WAG ratio. Figure 5.9 is a plot of the TRF curves indicating maximum TRF of 56 after 0.4 PV of cumulative gas injection for 1:1 WAG compared to 81.3 at 0.6 PV gas injection for 1:2 WAG ratio. The two figures emphasize the feasibility of 1:2 WAG ratio at 0.2 PV for Saudi light crude-synthetic formation brine fluid pair. It is worth mentioning that comparing the two sets of experiments conducted using the two fluid pairs (n-Decane-brine and Saudi light crude-formation-brine) indicates that similar pore volumes of gas are injected in both decided optimum flooding scenarios (1:1 WAG at 0.4 PV slug size with n-decane and 1:2 WAG at 0.2 PV slug size with Saudi light crude oil).

To examine the combined effect of WAG parameters (WAG ratio and slug size) and to determine the best combination of the two parameters, the oil recovery factor and TRF for all the previously mentioned experiments at different combinations of WAG parameters for n-Decane-brine fluid pair were plotted in Figures 5.10 and 5.11.

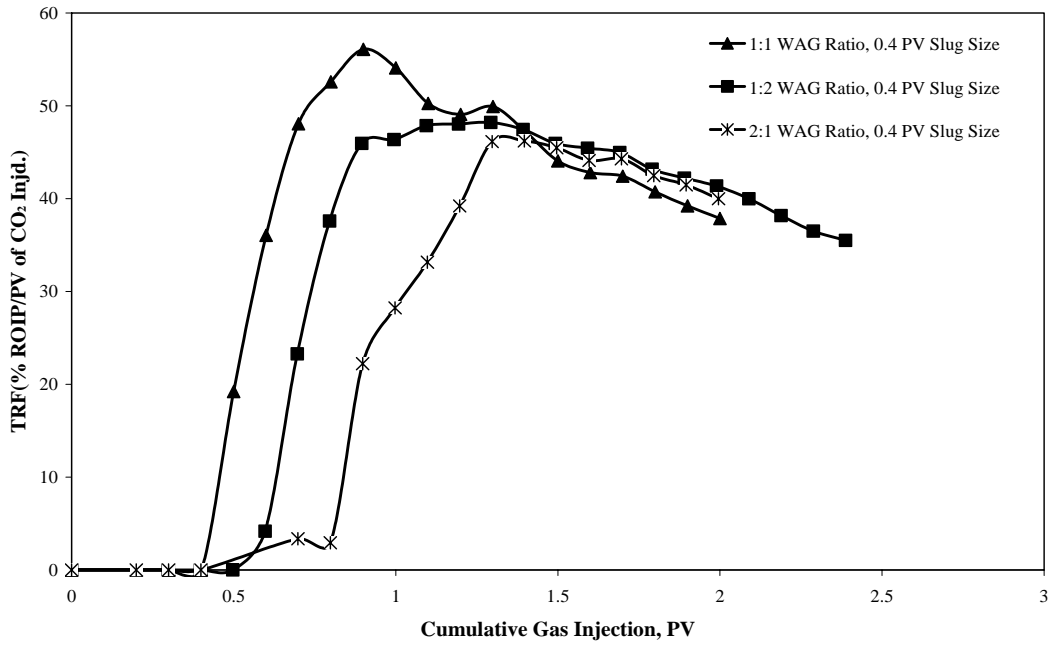


Figure 5.7: Effect of miscible WAG ratio on tertiary recovery factor for 0.4 PV slug size displacement experiments using n-Decane-brine fluid pair.

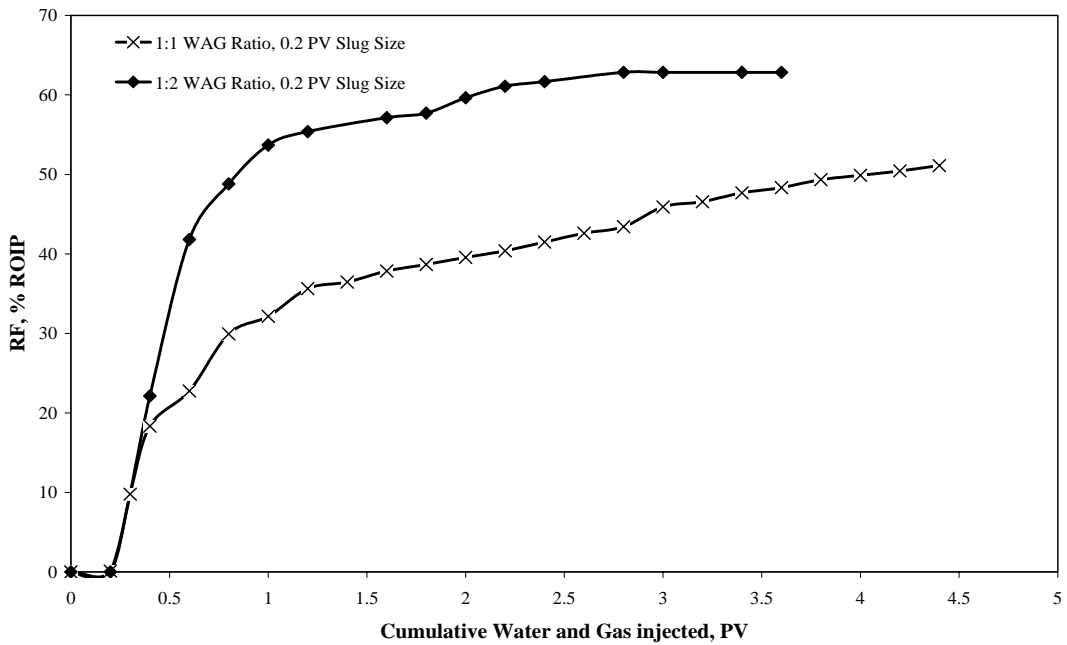


Figure 5.8: Effect of miscible WAG ratio on recovery factor for 0.2 PV slug size displacement experiments using Saudi light crude-synthetic formation brine fluid pair.

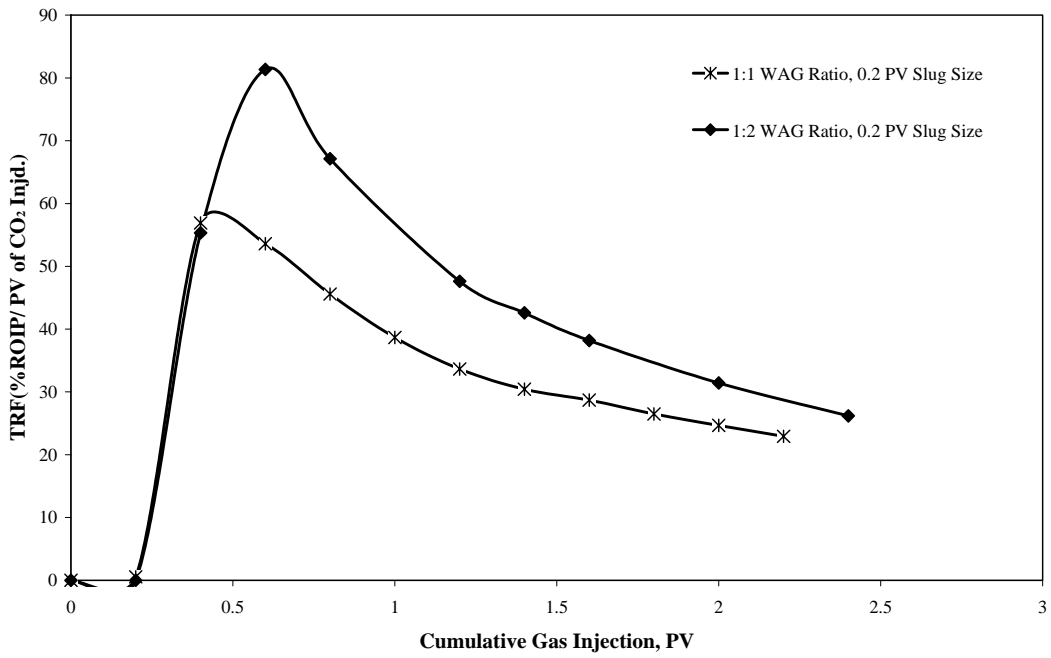


Figure 5.9: Effect of miscible WAG ratio on tertiary recovery factor for 0.2 PV slug size displacement experiments using Saudi light crude-synthetic formation brine fluid pair.

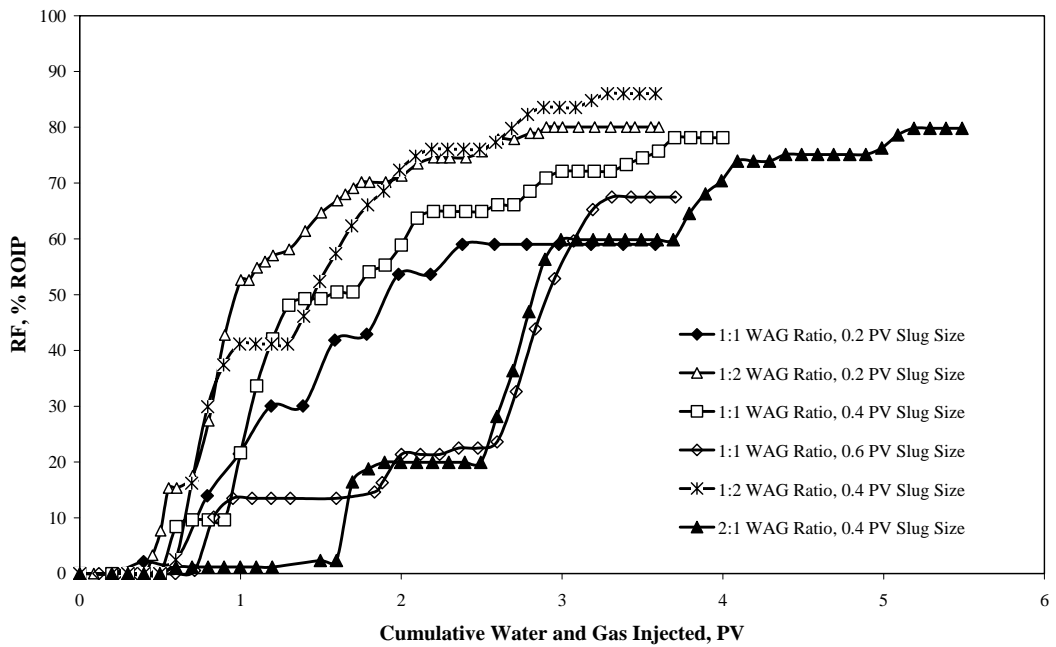


Figure 5.10: Effect of miscible WAG Parameters on recovery factor for n-Decane-brine fluid pair.

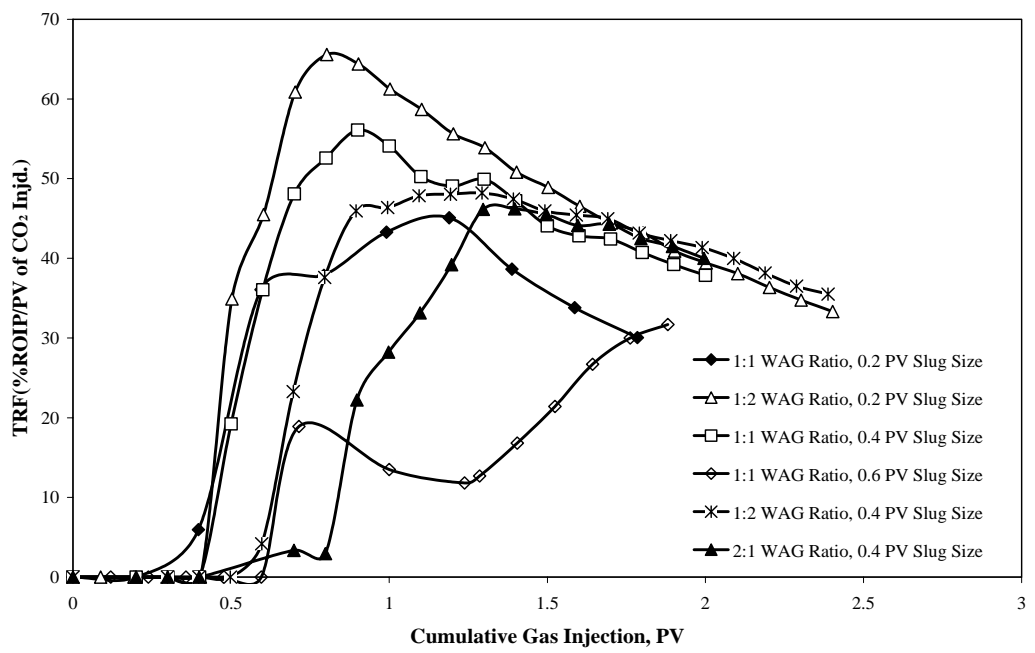


Figure 5.11: Effect of miscible WAG Parameters on tertiary recovery factor for n-Decane-brine fluid pair.

The figures indicate that 1:2 WAG flooding at 0.2 PV slug size seems to be the best flooding scenario based on the higher recovery obtained corresponding to the amount of gas injection.

CO₂ utilization factor (UF) is commonly used to evaluate field projects and is defined as the volume of gas injected at standard conditions for each barrel of oil produced. Figure 5.12 is a bar chart of the calculated UF (MSCF/bbl), TRF and recovery factor (% ROIP) at different cumulative pore volumes of gas injection (0.5, PV at maximum TRF, and 1.8 PV) for all runs. The figure verify that 1:2 WAG ratio at 0.2 PV slug size is the best flooding scenario. This support the output obtained from the recovery factor and TRF curves mentioned previously. The output of 1:2 WAG ratio at 0.2 PV slug size agrees with that obtained for 1:1 WAG ratio at 0.4 PV slug size since both experiments experienced similar injection volumes of gas. 1:1 WAG ratio at 0.6 PV does not seem to be economically feasible and it yields the least recovery and tertiary recovery factors and consumes the highest gas volume among all the runs conducted.

5.3 Secondary versus Tertiary WAG Injection

Miscible WAG flooding was performed at OOIP to investigate and compare the feasibility of the secondary WAG flooding at higher oil saturation compared to the conventional tertiary WAG flooding implemented subsequent to water flooding. This was conducted using n-Decane-brine fluid pair and WAG parameters were selected based on the interpretation of the previous runs, which showed that 1:2 WAG ratio and 0.2 PV slug size is the optimum WAG parameters. Figure 5.13 is a plot of the obtained recovery factor curves for both flooding processes at the same WAG ratio and slug size combination. The figure shows a good ultimate recovery factor of 90 % PV for the secondary gas injection process compared to 63.1 % PV for the tertiary recovery process. High water saturations shield residual oil from injected solvent in tertiary gas floods. Therefore, the higher recovery factor obtained for the secondary WAG is attributed to the less volume of brine present as connate water subsequent to the secondary process.

TRF defined this time as

$$TRF = (RF (\% OOIP)/Gas\ injected\ (PV)).....(5.2)$$

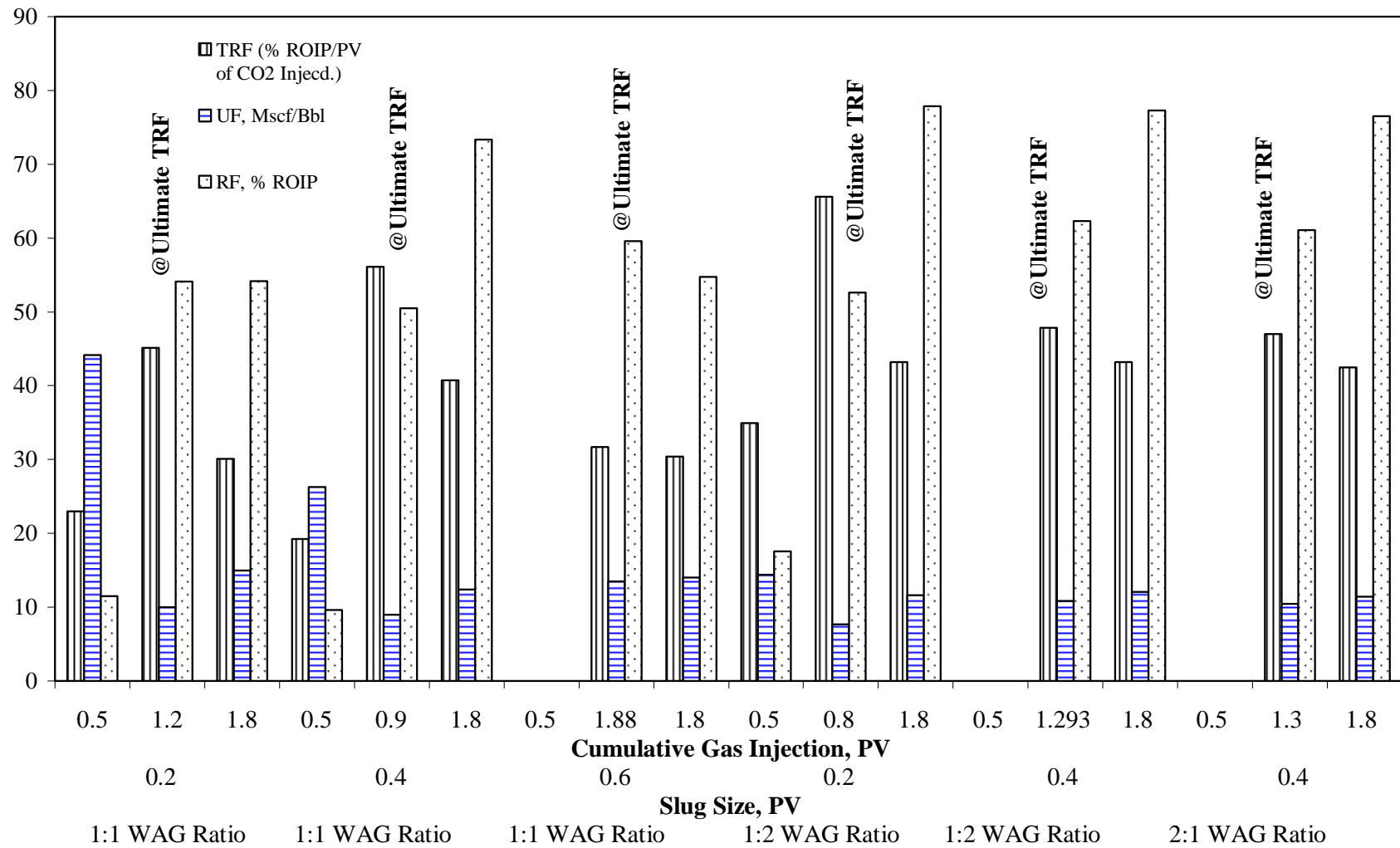


Figure 5.12: CO₂ Utilization Factor, tertiary recovery factor, and recovery factor of different miscible WAG parameters for n-Decane-brine fluid pair.

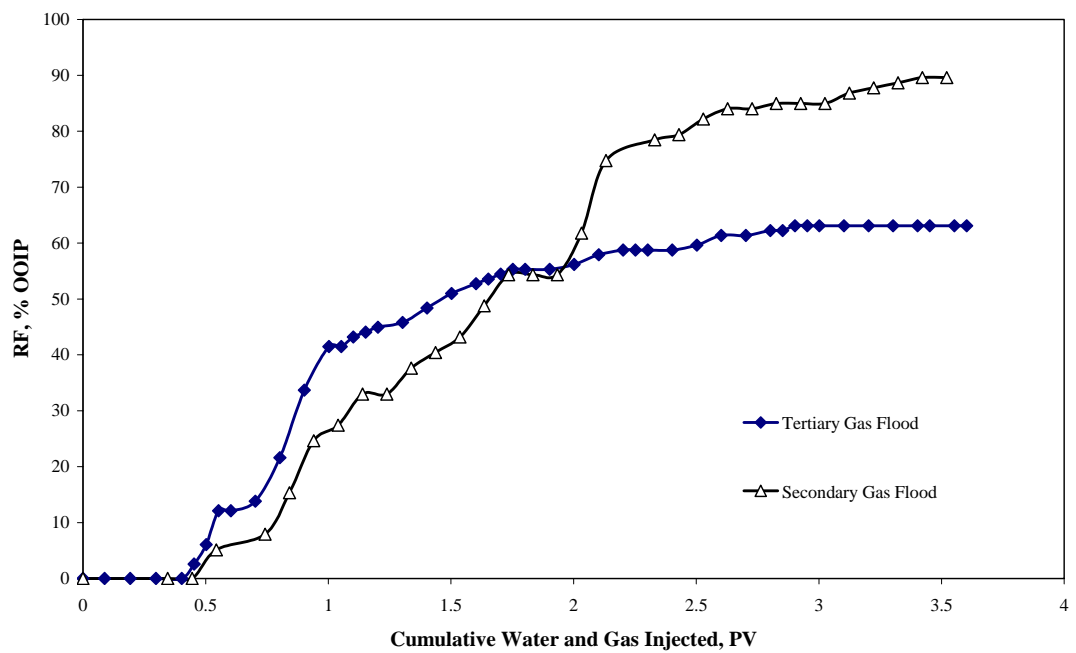


Figure 5.13: Recover factor in percentage of initial oil in place for secondary and tertiary gas injection using n-Decane-brine fluid pair.

was used and the curves of the two runs conducted were compared in Figure 5.14. The figure indicates an appreciable delay in approaching maximum TRF of 48.7 for the secondary process obtained after a cumulative gas injection of 1.55 PV compared to 52.6 approached after 0.8 PV of gas injection for the tertiary process. Therefore, secondary gas flooding process is good in term of ultimate recovery but it requires larger amount of gas particularly early in the injection process.

5.4 Effect of Brine Composition

Literature shows some disagreement on the effects of brine composition on oil recovery. Kwan et al. [75] concluded that oil recovery is independent of brine composition. On the other hand, other researchers [76-78] indicated that changes in brine composition could have a large effect on oil recovery. Water flooding and core imbibition experiments conducted by Tang and Morrow [78] with 1% solutions of NaCl, CaCl₂ and AlCl₃ showed increased recoveries (forced displacement) and decreased (natural) imbibition rates with the increase in cation valency. In contrast, Filoco and Sharma [79] conducted centrifuge experiments on Berea cores and found that oil recovery via imbibition increases significantly with increasing salinity of connate brine.

To investigate the effect of salinity and brine composition on oil recovery of miscible WAG injection, two experiments were conducted using n-Decane and two brine compositions, a saline solution composed of 2.55% NaCl and 0.45% CaCl₂ named brine and another higher salinity solution, designated as synthetic formation brine, representing the Saudi reservoir formation brine composed of 5.89 % NaCl, 2.24% CaCl₂ and 0.15% MgCl₂. Figure 5.15 is a plot of the recovery factor curves for both runs. The figure indicates an equal ultimate recovery of 80.0 % ROIP with some delay in approaching that recovery when using the low salinity brine solution. TRF curves of the runs conducted with different brines were plotted in Figure 5.16. A maximum TRF of 65.6 was obtained for low salinity brine after a cumulative gas injection of 0.8 PV compared to 106.0 after 0.5 PV of gas injection for synthetic formation brine. The early approach of the ultimate recovery when using synthetic formation brine could be attributed to the rock/fluid system interactions that may alter the rock surface wettability to more water wet condition in

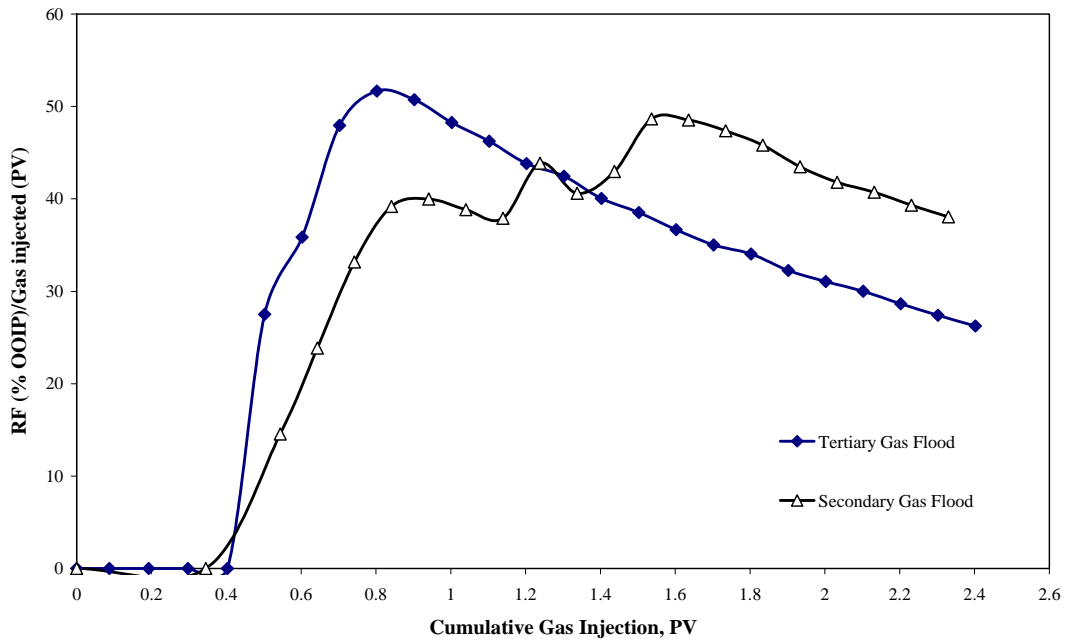


Figure 5.14: Tertiary recovery factor of tertiary versus secondary miscible gas injection using n-Decane-brine fluid pair.

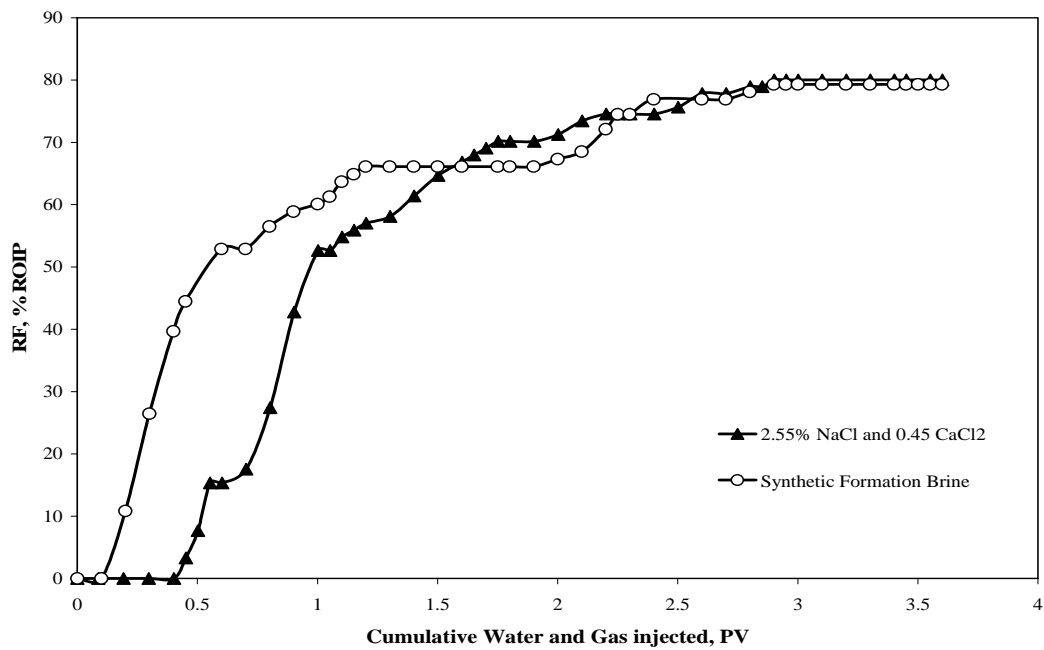


Figure 5.15: Effect of brine composition on n-Decane recovery factor of miscible flooding at 1:2 WAG ratio, 0.2 PV slug size.

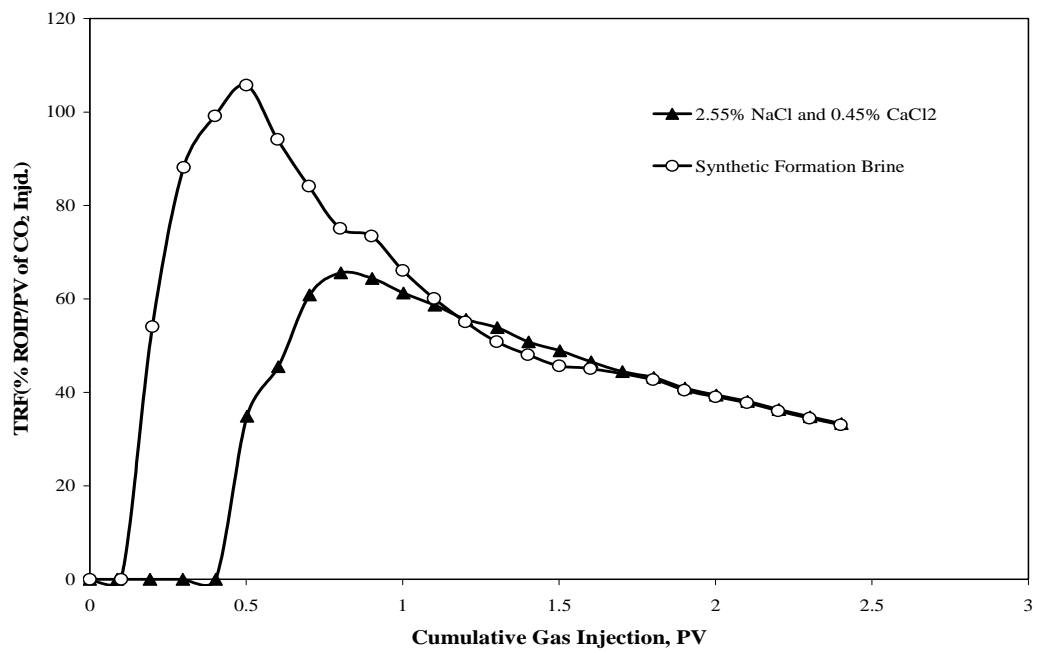


Figure 5.16: Effect of brine composition on n-Decane tertiary recovery factor of miscible flooding at 1:2 WAG ratio, 0.2 PV slug size

presence of higher concentration of multivalent cations like Ca^{++} and Mg^{++} . This behavior of higher recovery with increasing salinity was also observed during the secondary water flooding process where recovery obtained was 24 % OOIP when using synthetic formation brine compared to 21 % for low salinity brine.

5.5 Effect of Oil Type and Viscosity

To investigate the effect of viscosity and oil composition on oil recovery, n-Decane mineral oil, Saudi light crude oil, and Saudi medium crude oil all with synthetic formation brine were used in three WAG flooding runs at 1:2 WAG ratio with 0.2 PV slug size. The WAG parameters were chosen based on the interpretation of the previous runs. Figure 5.17 is a plot of the obtained oil recovery curves for the three runs after cumulative alternating water and gas injection of 3.6 PV. The run with n-Decane shows the highest oil recovery of 79.3 % ROIP followed by the Saudi light and then the Saudi medium crude oils with 62.8 % and 51.2 % ROIP respectively.

TRF curves of the runs conducted with different oils are plotted in Figure 5.18. The figure indicates a maximum TRF of 105.8 for n-Decane after 0.5 PV of cumulative gas injection, followed by 81.3 for Saudi light crude at 0.6 PV and finally 67.6 for Saudi medium crude oil at 0.5 PV of cumulative gas injection.

The decreasing recovery with increasing oil viscosity is attributed to viscous fingering and dispersive bypassing as stated by Stern [80]. The low mobility ratio of the displacement process during the gas slug injection adversely affects the sweep efficiency. The findings agree with that of Kremesec and Sebastian [81] in their miscible CO_2 flooding work of three reservoir oils where they concluded that CO_2 breakthrough time was found to decrease and residual oil saturation to increase as oil to gas viscosity ratio increases. In addition, capillary tube visual cell studies by Yeh et al [82] and displacement studies in oil wet, intermediate and water wet cores using solvent and three reservoir oils by Rao et al [83] show that miscible gas flooding may induce wettability alteration where water wet surfaces become strongly oil wet when in contact with swelling oil.

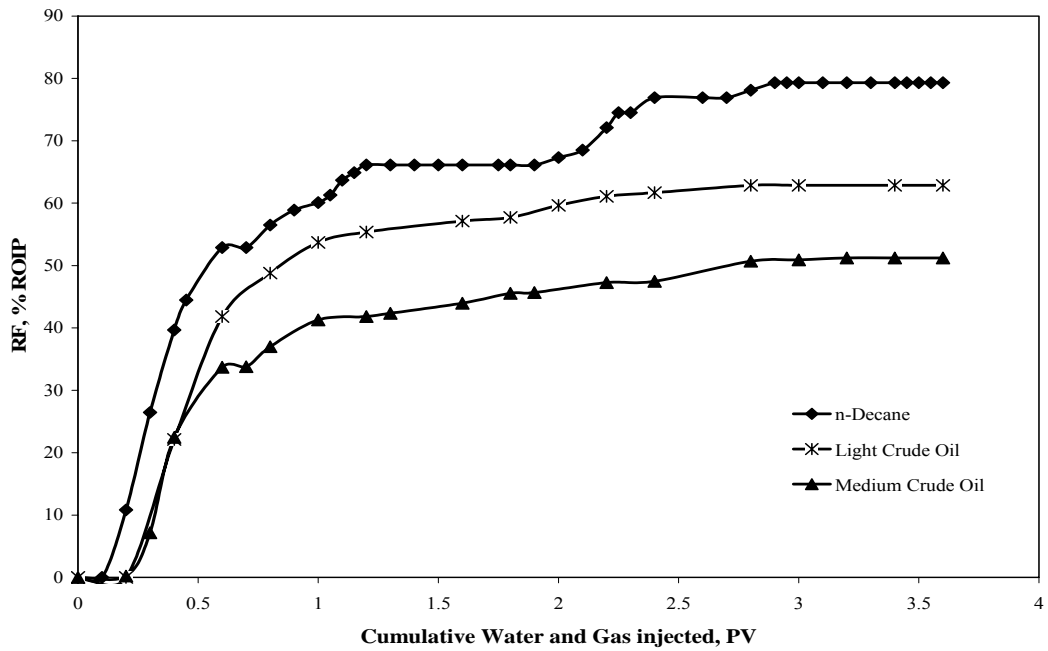


Figure 5.17: Effect of oil type on recovery factor of miscible flooding at 1:2 WAG ratio, 0.2 PV slug size.

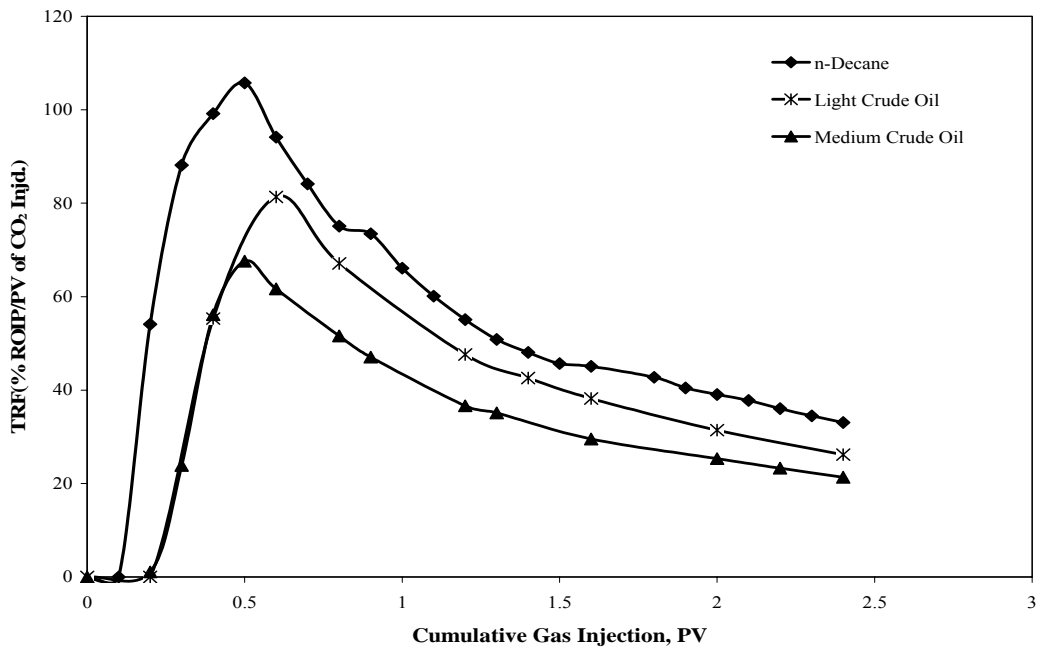


Figure 5.18: Effect of oil type on tertiary recovery factor of miscible flooding at 1:2 WAG ratio, 0.2 PV slug size.

This may explain the substantial decreasing oil recovery of the two experiments with crude oils compared to that of the mineral n-Decane, which is known to be non-effective in terms of wettability alteration. Similarly as oil API differs as in the case of the light and medium Saudi crude oils, heavier components content increases and induced asphaltene deposition will occur with the heavier crude near the injection end affecting the rock wettability converting it towards more oil wet condition and hence decreasing injectivity and consequently oil recovery.

5.6 Effect of Core Orientation

Gravity determines the segregation of the reservoir fluids and hence controls the vertical sweep efficiency of the displacement process. Gravity-stable displacements of oil by gas injection or WAG in dipping reservoirs as secondary or tertiary process results in very high oil recovery. This has been confirmed by laboratory tests, pilot tests as well as field applications [41, 84-90]. Although the purpose of WAG injection is to mitigate the gravity segregation effects and provide a stable injection profile, WAG in down dip reservoirs have shown better profile control and higher recoveries. Hence, the gravity considerations in WAG design are important

Gravity effect was studied by comparing two experiments using vertical and horizontal core orientations. Saudi light crude-synthetic formation brine fluid pair was used with WAG ratio of 1:2 at 0.2 PV slug size. The water and gas injection in the vertically mounted core was made from bottom to top simulating the injection process in up dipped reservoirs. The oil recovery and tertiary recovery factor were compared with the previous run conducted with the same fluid pair in horizontally laid core. Figure 5.19 shows ultimate oil recovery of 62.8 % ROIP for horizontally laid core compared to lower recovery of 47.5% ROIP for the vertically mounted core. This difference can be attributed to the gravity induced fingering of gas towards the outlet end of the core bypassing in the way up portion of the oil trapped in rock sample pore spaces. This observation agrees with the well-known phenomena of the gravity segregation on oil recovery by gas injection. TRF curves of the two runs conducted were plotted in Figure 5.20. The figure indicates a TRF of 81.3 after 0.6 PV of cumulative gas injection for horizontally laid core

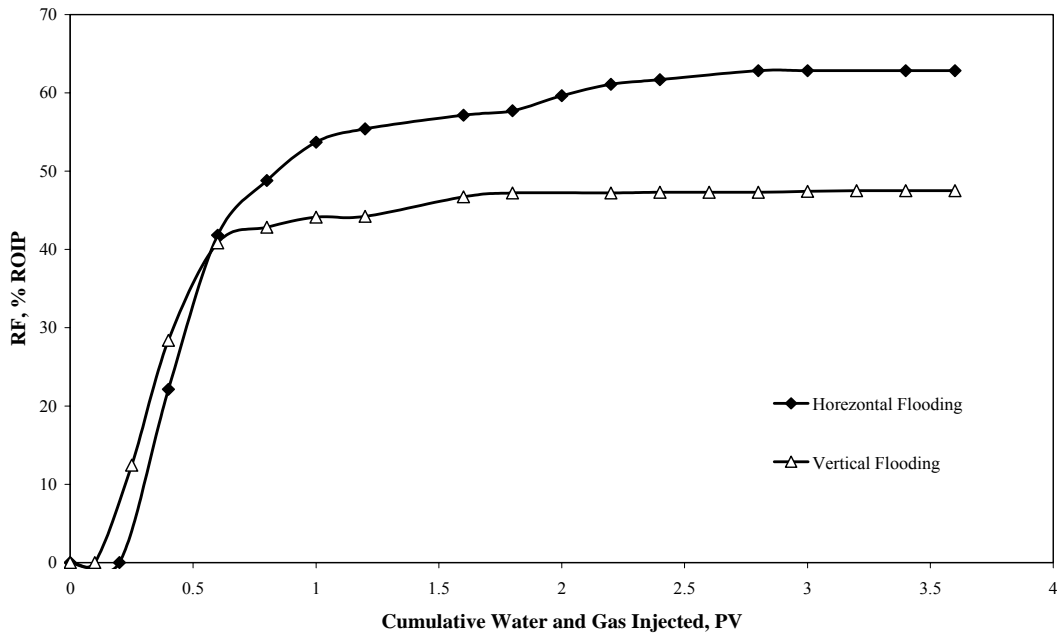


Figure 5.19: Effect of core orientation on recovery factor of miscible flooding at 1:2 WAG ratio, 0.2 PV slug size using Saudi light crude-synthetic formation brine fluid pair.

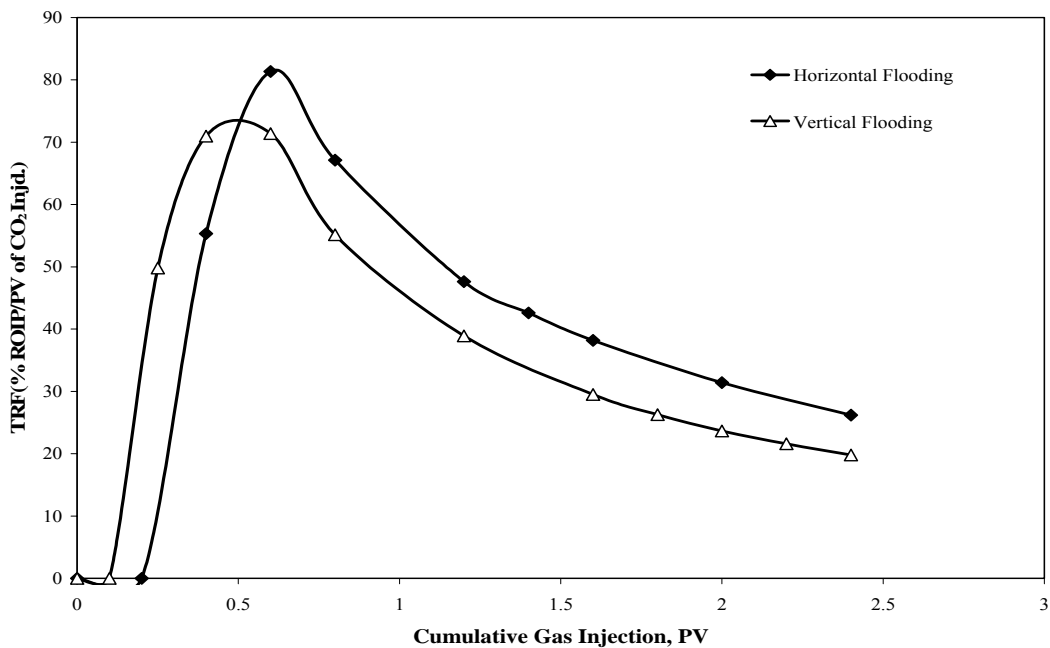


Figure 5.20: Effect of core orientation on tertiary recovery factor of miscible flooding at 1:2 WAG ratio, 0.2 PV slug size using Saudi light crude-synthetic formation brine fluid pair.

compared to 73.0 after 0.5 PV of gas injection for the vertically mounted core.

5.7 Effect of Core Length

Gravity segregation is dominant in any gas tertiary recovery process. Warner [73] indicated that gravity segregation dominates quite rapidly and only 10 % of near injector area is fully swept by gas. To investigate the effect core length on WAG flooding process two experiments were conducted on 2 and 4 ft long cores using Saudi light crude oil-synthetic formation brine fluid pair with WAG ratio of 1:2 at 0.2 PV slug size. Recovery curves plotted in Figure 5.21 indicates a close ultimate recovery factor of 61.9 and 62.8 % ROIP for 4 and 2 ft core lengths respectively therefore core length was not a significant factor in our case. Small delay has been noticed in approaching the ultimate recovery for the two feet core sample.

Rathmell et al. [41] studied the effect of core length on oil recovery by miscible CO₂ flooding. He indicated that both ultimate and breakthrough recoveries increase with the increase of core length, Rathmell et al [41] work covered high range of core lengths from 6.0 to 42.5 ft which is not the case in our work. Figure 5.22 shows a maximum TRF of 101 at 0.5 PV of gas injection for the 4 ft long core and a lower TRF of 81.3 after 0.6 PV of gas injection for the 2 ft long core. Based on the TRF, it is clear that flooding process in 4 ft core is better than the 2 ft core. Practically, long core tests are not only appropriate and useful but also essential to examine the actual effect of gravity segregation on WAG injection process.

5.8 CGI versus WAG Injection Mode

WAG injection process are conducted to decrease the gas mobility maintaining pressure and saving operation cost of gas injection with inexpensive water injection. Ideally, gas provides miscibility while water improves sweep efficiency. Several studies [14, 21, 65, and 88] indicated that CGI is more efficient than WAG injection in water wet porous media due to water blockage during CO₂ flooding. To investigate this, CGI experiment was conducted using n-Decane-brine fluid pair and compared with that conducted with the selected best WAG parameters (1:2 WAG ratio, 0.2 PV slug size) using the same fluids.

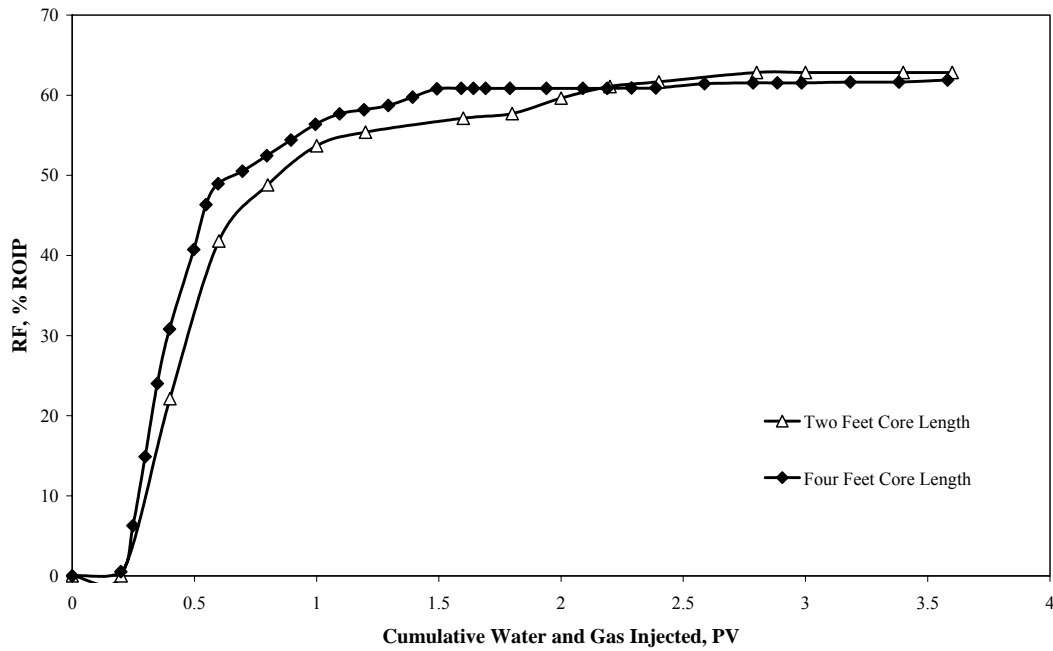


Figure 5.21: Effect of core length on recovery factor of miscible flooding at 1:2 WAG ratio, 0.2 PV slug size using Saudi light crude-synthetic formation brine fluid pair.

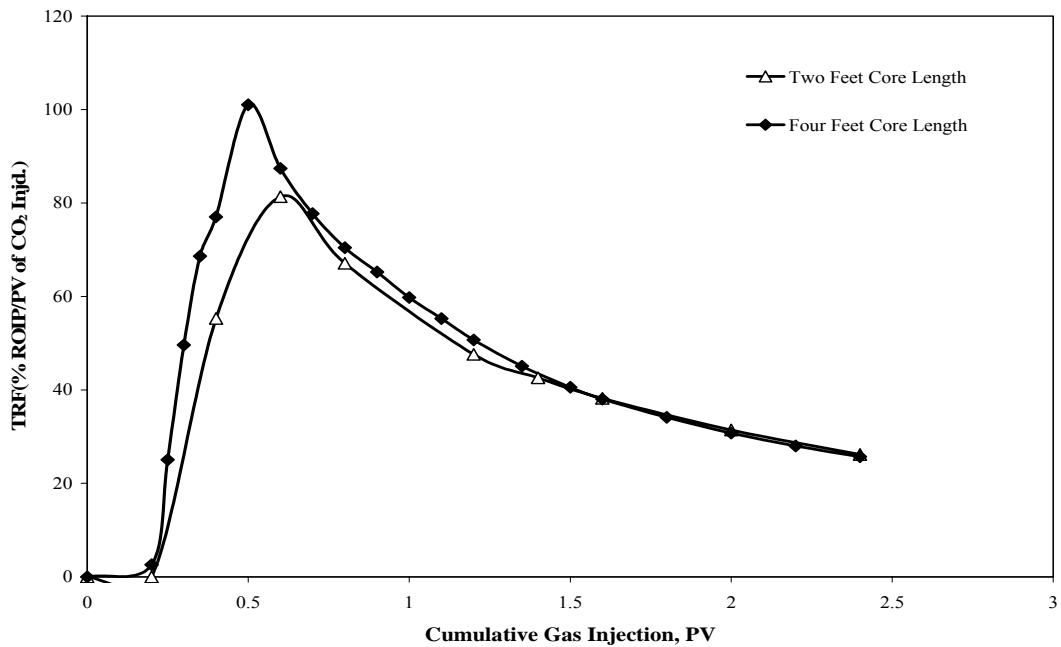


Figure 5.22: Effect of core length on tertiary recovery factor of miscible flooding at 1:2 WAG ratio, 0.2 PV slug size using Saudi light crude oil- synthetic formation brine fluid pair.

Figure 5.23 is a plot of the oil recovery factor curves for the two experimental runs. The data obtained shows an ultimate recovery of 96 % ROIP for CGI compared to 80 % ROIP for WAG injection mode corresponding to 68.8 % and 63.1 % OOIP respectively. This indicates that CGI appears to have performed better than WAG injection in term of recovery. Berea core samples used in this work are known to be strongly water wet. In addition, mineral oil used as oleic phase is known to be non wetting. Therefore, such observation, agrees well with the previous mentioned observations on the efficiency of CGI in water wet porous media.

TRF curves for the two experimental runs were plotted in Figure 5.24. The figure indicates that maximum TRF of 71.7 was reached for CGI after 0.7 PV of gas injection compared to 65.6 for WAG injection after 0.8 PV of gas injection. It should be noted the CGI floods utilize more volume of CO₂ than WAG. Hence, a valid comparison of the two should be based on utilization factor (UF). Figure 5.25 is a plot of the utilization factor for the two experimental runs and it indicates that the application of the continuous CO₂ flood consumes higher gas volume to reach such higher recovery. This implies that WAG injection seems to be more feasible economically.

It is important to note that the conclusions from recovery and tertiary recovery factor plots are contradictory with that of utilization factor. This suggests the use of CGI up to the peak TRF and later switches over to WAG process to maximize recovery with minimum gas volume injection. This seems to be the principle behind the patented processes of Hybrid WAG and Denver Unit WAG of UNOCAL and Shell respectively.

For more investigation, CGI experiment was conducted on 4 ft long core using Saudi light crude oil-synthetic formation brine fluid pair and compared with that conducted at selected best WAG parameters (1:2 WAG ratio, 0.2 PV slug size) using the same fluids and core length. Figure 5.26 shows the recovery curves for the two experimental runs. The figure indicates a higher recovery of 62.8 % ROIP for WAG mode compared to 46.8 % ROIP for CGI modes. The reversal trend seen in these two experiments compared to the above mentioned experiments conducted at 2 ft core using n-Decane and low salinity brine

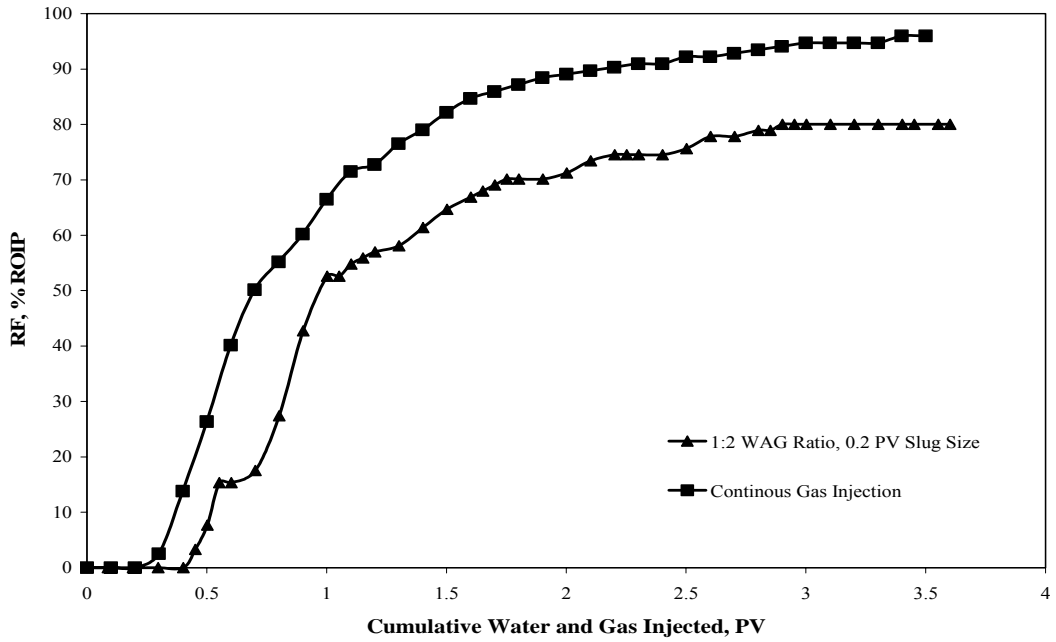


Figure 5.23: Effect of miscible injection mode on recovery factor using n-Decane-brine fluid pair.

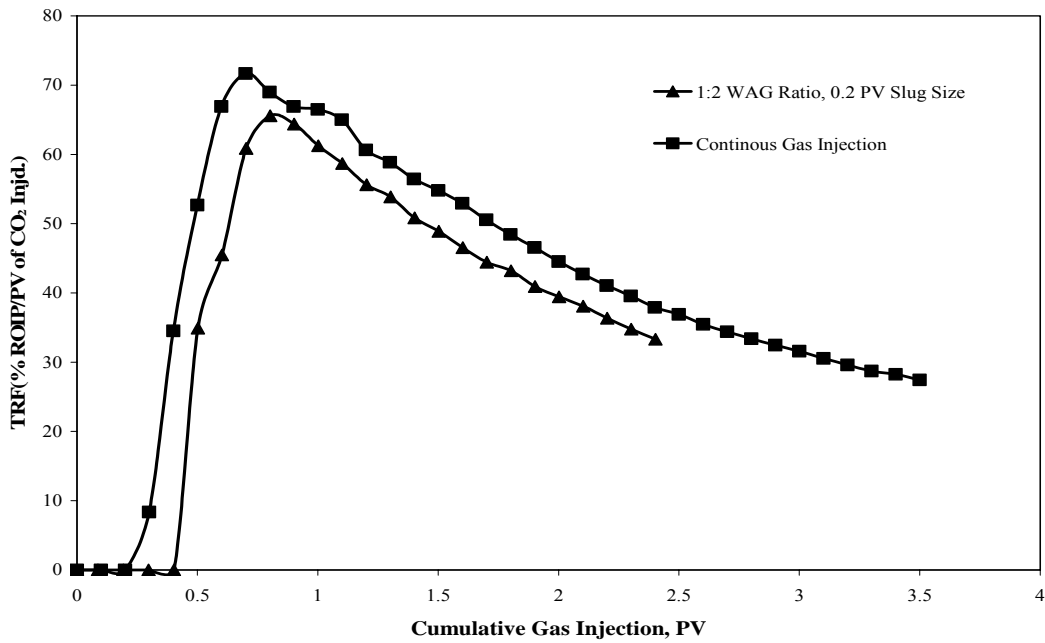


Figure 5.24: Effect of miscible injection mode on tertiary recovery factor using n-Decane-brine fluid pair.

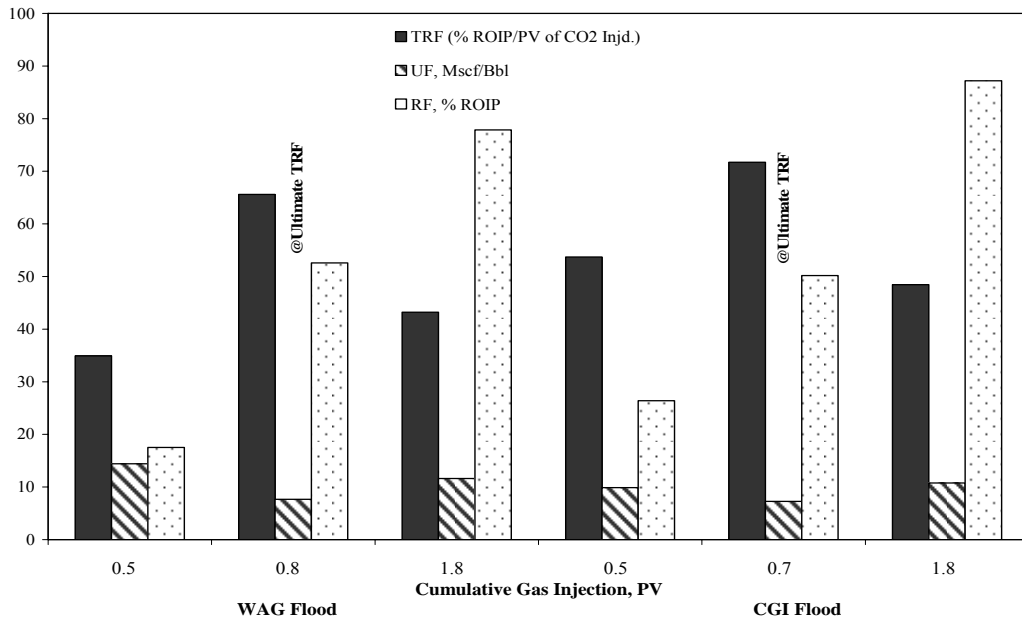


Figure 5.25: CO₂ Utilization Factor, tertiary recovery factor, and recovery factor of CGI and WAG injection mode for n-Decane-brine fluid pair.

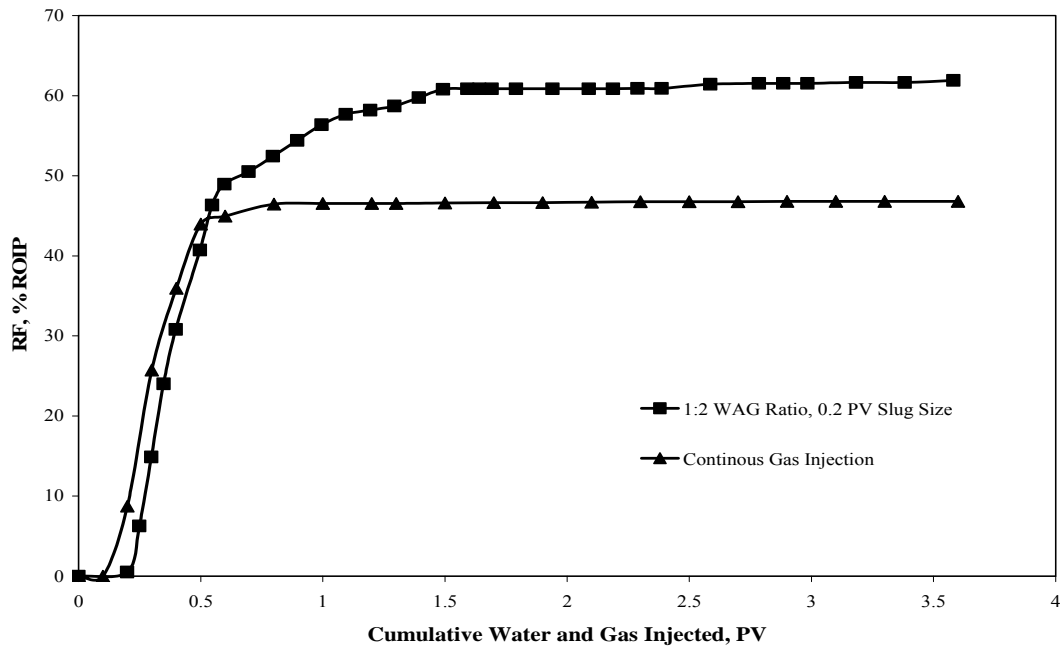


Figure 5.26: Effect of miscible injection mode on recovery factor using Saudi light crude-synthetic formation brine fluid pair on 4 ft long core.

fluid pair is due to the effect of the presence of Saudi light crude oil which is believed to alter the rock wettability towards oil wet condition preventing the water blockage during the WAG process. TRF curves are plotted in Figure 5.27 and indicate an ultimate TRF of 101 at 0.5 PV of gas injection for WAG injection mode compared to 89.9 % accomplished after 0.4 PV of gas injection for the CGI mode.

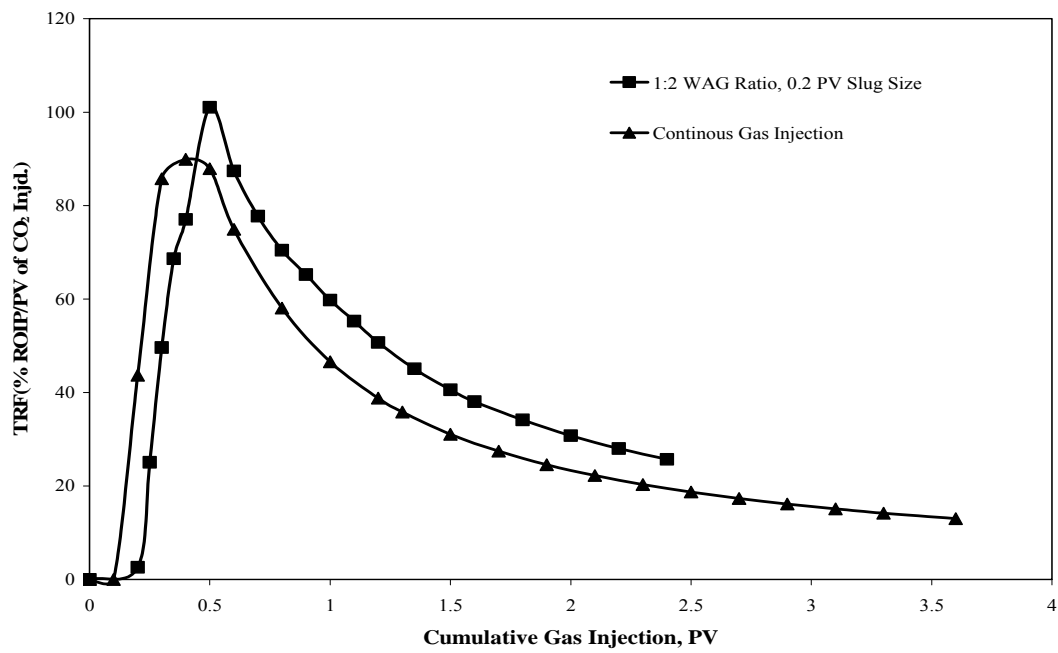


Figure 5.27: Effect of miscible injection mode on tertiary recovery factor using Saudi light crude-synthetic formation brine fluid pair on 4 ft long core.

CHAPTER 6

CONCLUSIONS AND RECOMMENDATIONS

Miscible CO₂ flooding process was conducted at different parameters. These parameters included injection scheme (CGI and WAG), WAG ratio, slug size, oil composition and viscosity, brine composition, core length and core orientation. In addition, CO₂ flooding as a secondary process was investigated and compared to the conventional tertiary gas flooding. Based on the results obtained, the following conclusions were drawn:

1. Miscible CO₂ flooding experiments at different WAG ratio and slug size show that 1:2 WAG ratio at 0.2 PV slug size is found to be the best combination delivering the highest recovery and tertiary recovery factors.
2. Comparison of the miscible WAG flooding as a secondary process to the conventional tertiary miscible WAG flooding process shows that secondary miscible WAG flooding process is better in term of higher ultimate recovery. However, secondary WAG requires larger amount of gas injection particularly in the early injection process, this may be attributed to the less water saturation present as connate water compared to the higher water saturation accumulated subsequent to the normal water flooding secondary process.
3. Equal ultimate recovery were obtained for the miscible WAG experiments conducted at the best flooding scenario with different brine composition and concentration with some delay in approaching that recovery when using the low salinity brine solution. An increase in the tertiary recovery factor and slight decrease in the UF was noticed as we switch from low to high salinity brine.
4. As the oleic phase API decreases and the viscosity increases, recovery factor and tertiary recovery factor decreases due to wettability alteration and viscose fingering for both miscible and immiscible injection modes.
5. Gravity determines the segregation of the reservoir fluids and hence controls the vertical sweep efficiency of the displacement process. Gravity-stable displacements of oil by miscible WAG injection in vertically mounted core

representing up dipping reservoirs resulted in slightly lower oil recovery than that obtained for horizontally laid core.

6. Comparison between different core lengths at miscible WAG flooding process shows that close ultimate recovery factor were obtained for 2 and 4 ft core lengths. Small delay has been noticed in approaching the ultimate recovery for the two feet core sample.
7. The comparison between Miscible CGI and WAG injection modes using n-Decane-brine fluid pair shows that miscible CGI appears to have better performance than miscible WAG injection in term of recovery. Berea core samples used in this work are known to be strongly water wet. In addition, mineral oil, used as oleic phase, is known to be non wetting. Therefore, such observation, agrees well with the previous mentioned observation on the efficiency of CGI in water wet media. However, larger amount of gas injection is needed. Therefore, it is not considered feasible from economical point of view.
8. Miscible CGI and WAG injection modes using Saudi light-synthetic formation brine fluid pair shows a higher recovery for CGI modes. The reversal trend seen in these two experiments compared to the experiments conducted core using n-Decane-brine fluid pair is due to the presence of Saudi light crude oil which may alter the rock wettability towards oil-wet condition preventing the water blockage during the WAG process.
9. The decision on the best WAG ratio should be decided based on the economics taking into consideration both the incremental oil recovery and the cost and availability of CO₂

Based on the work conducted and conclusions reached, the following recommendations are suggested:

1. For more realistic and representative work of the local reservoirs, more experiments are to be conducted using live crude oil and samples representing Saudi reservoirs.
2. Simulation of the conducted experiments using available simulators will help in investigating more parameters and up scaling the work to field scale.

3. Hybrid-WAG flooding should be conducted on long cores to determine the optimum mode for gas floods and to compare their effectiveness against gravity-stable gas floods.

NOMENCLATURE

ANN	: Artificial Neural Network
API	: oil gravity °API
C_i	: carbon number
Exp. No.	: experiment numbers
F	: weighting composition parameter
F_R	: mole percent C_2 through C_6 in the reservoir fluid, %
Interm.	: intermediates components, C_1 - C_4 , H_2S , and CO_2 , fraction
K_i	: normalized partition coefficient for carbon number i .
MF_i	: critical temperature modification factor of injected gas component i .
$M_{inj.}$: molecular weight of the injected gas
MMP_{pure}	: CO_2 -oil Minimum Miscibility Pressure, MPa
MMP_{impure}	: Flue gas-oil Minimum Miscibility Pressure, MPa
$MW_{C_{5+}}$: molecular weight of C_{5+} fraction
$MW_{C_{7+}}$: molecular weight of C_{7+} fraction
$P_{C, pure}$: CO_2 critical pressure, MPa
P_{Ci}	: critical pressure of the gas component i , MPa
$P_{C, inj.}$: injection gas critical pressure, MPa
P_{CW}	: weight average pseudocritical pressure, MPa
$P_{r, pure}$: reduced CO_2 minimum miscibility pressure, fraction
$P_{r, impure}$: reduced flue gas minimum miscibility pressure, fraction
SF_i	: Dong (1999) factor representing the strength of species i in changing the apparent critical temperature of the mixture relative to the critical temperature of CO_2
T_{ac}	: mole average pseudocritical temperature with using factor SF_i , °K
T_{C, CO_2}	: critical temperature of pure CO_2 gas, °C
$T_{C, inj.}$: injected gas critical temperature, °K

T_{ci}	: critical temperature of gas component i, °C
T_{Ci}	: critical temperature of gas component i, °K
T_{CM}	: mole average critical temperature, °K
T_{CW}	: weight average pseudocritical temperature with using the Multiplying factor (MF_i), °C
T_{pc} °C	: Pseudocritical temperature (may be weight average or mole average), °C
T_R	: reservoir temperature, °C
Vol.	: volatiles (C_1 and N_2) mole percentage, %
w_i	: weight fraction of gas component i
w_{ic2+}	: component i normalized weighting fraction in the C_2+ fractions of crude oil
x_{CO_2}	: CO_2 mole percentage in the injection gas, %
x_i	: mole fraction of gas component i
y	: mole fraction of diluted component
ρ	: oil gravity °API
ρ_{MMP}	: CO_2 density at MMP, g/cm^3
Σ	: sum operator

REFERENCES

1. Benson S. and Peter Cook, “Carbon Dioxide Capture and Storage”, Chapter 5, Intergovernmental Panel on Climate Change Report, Cambridge University Press, 2005.
2. Oen, P. M., “The Development of the Greater Gorgon Gas Fields”, The APPEA Journal, 43(2), pp.167–177, 2003.
3. Van der Meer, L.G.H.; Hartman, J.; Geel, C.; and E. Kreft, “Re-injecting CO₂ into an Offshore Gas Reservoir at a Depth of Nearly 4000 metres Sub-Sea”, Proceedings of the 7th International Conference on Greenhouse Gas Control Technologies (GHGT-7), September 5–9, Vancouver, Canada, Vol. I, 521-530, 2004.
4. Bachu, S. and Haug, K., “In-Situ Characteristics of Acid –Gas Injection Operations in the Alberta Basin, Western Canada: Demonstration of CO₂ Geological Storage, Carbon Dioxide Capture for Storage in Deep Geologic Formations – Results from the CO₂ Capture Project, v. 2: Geologic Storage of Carbon Dioxide with Monitoring and Verification”, S.M. Benson (ed.), Elsevier, London, pp. 867–876, 2005.
5. Freund, P., “Progress in Understanding the Potential Role of CO₂ Storage”, Proceedings of the 5th International Greenhouse Gas Conference Technologies (GHGT5), Cairns, Australia, 13–16 August, pp. 272–278, 2000.
6. Stevens, S.H.; Kuuskraa, V.K.; and Gale, J., “Sequestration of CO₂ in Depleted Oil and Gas Fields: Global Capacity and Barriers to Overcome”, Proceedings of the 5th International Greenhouse Gas Conference Technologies (GHGT5), Cairns, Australia, 13–16 August, 2000.
7. Gozalpour, F., Ren, S. R. , Tohidi, B., “CO₂ EOR and Storage in Oil Reservoirs” Oil & Gas Science and Technology – Rev. IFP, Vol. (60) , No. 3, pp. 537-546, 2005.
8. Moberg, R.; Stewart, D.B.; and Stachniak, D., “The IEA Weyburn CO₂ Monitoring and Storage Project. Proceedings of the 6th International Conference on Greenhouse Gas Control Technologies (GHGT-6), J. Gale and Y. Kaya (eds.), Kyoto, Japan, 219–224, 1–4 October 2002.

9. Law, D., "Theme 3: CO₂ Storage Capacity and Distribution Predictions and the Application of Economic Limits. In: IEA GHG Weyburn CO₂ Monitoring and Storage Project Summary Report 2000–2004, M. Wilson and M. Monea (eds.), Proceedings of the 7th International Conference on Greenhouse Gas Control Technologies (GHGT7), Volume III, p 151–209, 2005.
10. Moritis, G. "CO₂ Sequestration Adds New Dimension to Oil, Gas Production". Oil and Gas Journal, 101(9), pp. 71–83, 2003.
11. Holt, T.; Jensen, J. L.; and Lindeberg, E., "Underground Storage of CO₂ in Aquifers and Oil Reservoirs", Energy Conversion and Management, 36(6–9), pp. 535–538, 1995.
12. Bondor, P.L., "Applications of Carbon Dioxide in Enhanced Oil Recovery". Energy Conversion and Management, 33(5), pp. 579–586, 1992.
13. Martin, F.D. and Taber, J. J., "Carbon Dioxide Flooding", Journal of Petroleum Technology, 44(4), pp. 396–400, 1992.
14. Stalkup Jr., F.I., "Miscible Displacement. SPE Monograph Series," New York, pp. 12-14, 1983.
15. Sequeira, D. S., "Compositional Effects on Gas-Oil Interfacial Tension and Miscibility at Reservoir Conditions" Dissertation, Petroleum Engineering Dept., Louisiana State University, December 2006.
16. Tzimas, E.; Georgakaki, A., Garcia Cortes, C. and Peteves, S.D. "Enhanced Oil Recovery using Carbon Dioxide in the European Energy System" Report EUR 21895 EN, Institute for Energy, Petten, The Netherlands, December 2005.
17. Goodwear, S.G., "Subsurface Issues for CO₂ Flooding of UKCS Reservoirs" Trans. Ichem E, 81, Part A, 2003.
18. Moritis, G., "2000 Worldwide EOR Survey", Oil & Gas J., 45, March 2000.
19. Green, D.W. and Willhite, G.P., "Enhanced Oil Recovery," Society of Petroleum Engineers, SPE Textbook Series Vol. 6, Richardson, TX, USA, 2003.
20. Shokir, E.M. El-M., "CO₂-Oil Minimum Miscibility Pressure Model for Impure and Pure CO₂ Streams" Journal of Petroleum Science and Technology, (58), pp. 173–185, 2007.

21. Taber, J.J.; Martin, F.D.; and Seright, R.S., "EOR Screening Criteria Revisited - part 1: Introduction to Screening Criteria and Enhanced Recovery Fields Projects", SPE Reservoir Engineering, 12(3), pp. 189–198, 1997.
22. Kavscek, A.R., "Screening Criteria for CO₂ Storage in Oil Reservoirs", Petroleum Science and Technology, 20(7–8), pp. 841–866, 2002.
23. Shaw, J. C. and S. Bachu, "Screening, Evaluation and Ranking of Oil Reserves Suitable for CO₂ Flood EOR and Carbon Dioxide Sequestration", Journal of Canadian Petroleum Technology, 41(9), pp. 51–61, 2002.
24. Wang, Y., "Analytical Calculation of Minimum Miscibility Pressure," Dissertation for PhD degree, Stanford University, Department of Petroleum Engineering USA, 1998.
25. Kovarik, F. S., "A minimum Miscibility Pressure Study Using Impure CO₂ and West Texas oil systems: Data Base, Correlations, and Compositional Simulation," Paper SPE 14689 presented at the SPE Production Technology Symposium, Lubbock, Texas, USA, pp. 1-14, Nov. 1985.
26. Benham, A. L.; Dowden, W. E.; and Kunzman, W. J., "Miscible Fluid Displacement Prediction of Miscibility," JPT, pp. 229-237, Oct. 1960.
27. Holm, L. W.; and Josendal, V. A., "Effect of Oil Composition on Miscible-Type Displacement by Carbon Dioxide", SPE J., pp. 87-98, Feb. 1982.
28. Johnson, J. P.; and Pollin, J. S., "Measurement and Correlation of CO₂ Miscibility Pressures," SPE 9790, presented at the 1981 SPE/DOE Joint Symposium on Enhanced Oil Recovery held in Tulsa, Oklahoma, April 5-8, 1981.
29. Sebastian, H. M.; Wenger, R. S.; and Renner, T. A., "Correlation of Minimum Miscibility Pressure for Impure CO₂ Streams," Paper SPE 12648 presented at the 1984 SPE/DOE Symposium on Enhanced Oil Recovery, Tulsa, OK, Apr. 15-18.
30. Flock, D. L.; and Nouar, A., "Parameter Analysis on The Determination of The Minimum Miscibility Pressure in Slim Tube Displacements," Journal of Canadian Pet. Tech., pp. 80-88, Sept-Oct. 1984.
31. Kuo, S. S., "Prediction of Miscibility for The Enriched-Gas," Paper SPE 14152, presented at the SPE Annual Technical Conference and Exhibition, Las Vegas, USA, Sept. 1985.

32. Elsharkawy, A. M.; Poettmann, F. H.; and Christiansen, R.L., "Measuring Minimum Miscibility Pressure: Slim-Tube or Rising-Bubble Method?," Paper SPE 24114 presented at the 1992 SPE/DOE Eighth Symposium on Enhanced Oil Recovery, Tulsa, OK, April 22-24.
33. Zhou, D.; and Orr, F. M. Jr., "An analysis of Rising Bubble Experiments to Determine Minimum Miscibility Pressures," Paper SPE 30786 presented at the 1995 SPE Annual Technical Conference and Exhibition, Dallas, TX, Oct. 22-25, 1995.
34. Lake, L. W., "Enhanced Oil Recovery," Prentice Hall, New Jersey, 1989.
35. R. L. Christiansen; and K. H. Haines, "Rapid measurement of minimum miscibility pressure using the rising bubble apparatus," SPE Reservoir Engineering Journal, pp. 523-527, Nov. 1987.
36. Dong, M.; Huang, S.; Dyer, S. B.; and Mourits, F. M., "A comparison of CO₂ Minimum Miscibility Pressure Determinations for Weyburn Crude Oil," Journal of Petroleum Science and Engineering, Vol. 31, No. 1, pp. 13–22, 2001.
37. Johnson, J. P.; and Pollin, J. S., "Measurement and Correlation of CO₂ Miscibility Pressures," Paper SPE 9790 presented at the SPE/DOE Second Joint Symposium on Enhanced Oil Recovery, Tulsa, USA, pp. 269-281, 1981.
38. Alston, R. B.; Kokolis, G. P.; and James, C. F., "CO₂ Minimum Miscibility Pressure: A correlation for Impure CO₂ Streams and Live Oil Systems," SPEJ, Vol. 25, No. 2, pp. 268– 274, 1985.
39. Zuo, Y.; Chu, Ji.; Ke, S.; and Guo, T., "A study on The Minimum Miscibility Pressure for Miscible Flooding Systems," Journal of Petroleum Science and Engineering, Vol. 8, No. 3, pp. 315-328, 1993.
40. Emera, M. K; and Sarma, H. K., "Genetic Algorithm (GA)–Based Correlations Offer More Reliable Prediction of Minimum Miscibility Pressures (MMP) between The Reservoir Oil and CO₂ or Flue Gas," Paper presented at 6th Canadian International Petroleum Conference, Calgary, Alberta, Canada, pp. 1-17, June 2005.
41. Rathmell, J. J.; talkup, F. I. S; and Hassinger, R. C., "A laboratory Investigation of Miscible Displacement by Carbon Dioxide," Paper SPE 3483 presented at the

- 46th Annual Fall Meeting of the Society of Petroleum Engineers of AIME 6200, New Orleans, La., pp. 1-16, 1971.
42. Metcalfe, R. S.; and Yarborough, L., "Discussion," JPT, pp. 1436–1437, Dec. 1974.
43. Cronquist, C., "Carbon Dioxide Dynamic Displacement with Light Reservoir Oils," Proc., Fourth Annual U.S. DOE Symposium, Tulsa, USA, pp. 18-23, Aug. 1978.
44. Holm, L. W.; and Josendal, V. A., "Mechanisms of Oil Displacement by Carbon Dioxide," JPT, pp.1427-1436, Dec. 1974.
45. Lee, J. I., "Effectiveness of Carbon Dioxide Displacement Under Miscible and Immiscible Conditions," Report RR-40, Petroleum Recovery Inst., Calgary, March 1979.
46. Yellig, W. F.; and Metcalfe, R. S., "Determination and Prediction of CO₂ Minimum Miscibility Pressures," JPT, pp. 160– 168, Jun.1980.
47. Orr, F. M. Jr.; and Jensen, C. M., "Interpretation of Pressure-Composition Phase Diagrams for CO₂/Crude-Oil Systems," SPE Journal, pp. 485-497, Oct. 1984.
48. Glaso, O., "Generalized Minimum Miscibility Pressure Correlation," SPEJ, pp. 927– 934, Dec. 1985.
49. Orr, F. M. Jr.; and Silva, M. K., "Effect of Oil Composition on Minimum Miscibility Pressure-Part 2: Correlation," SPE Reservoir Engineering Journal, Vol. 2, No. 4, pp. 479– 491, 1987.
50. Huang, H. F.; Huang, G. H.; Dong, G. M.; and Feng, G. M., "Development of an Artificial Neural Network Model for Predicting Minimum Miscibility Pressure in CO₂ Flooding," Journal of Petroleum science and Engineering, Vo., 37, No., pp. 83-95, 2003.
51. Emera, M. K.; and Sarma, H. K., "Use of Genetic Algorithm to Estimate CO₂-Oil Minimum Miscibility Pressure-a Key Parameter in Design of CO₂ Miscible Flood," Journal of Petroleum science and Engineering, Vol. 46, No. 1, pp. 37-52, 2004.

52. Dong, M., "Task 3- Minimum Miscibility Pressure (MMP) Studies, in the Technical Report: Potential of Greenhouse Storage and Utilization through Enhanced Oil Recovery," Petroleum Research Center, Saskatchewan Research Council (SRC Publication No. P-10-468-C-99), 1999.
53. Eakin, B. E.; and Mitch, F. J., "Measurement and Correlation of Miscibility Pressures of Reservoir Oils," Paper SPE 18065 presented at 63rd Annual Technical Conference and Exhibition, Houston, TX, pp. 75-81, Oct. 1988.
54. Yuan, H.; Johns, R. T.; Egwuenu, A. M.; and Dindoruk, B., "Improved MMP Correlations for CO₂ Floods Using Analytical Gas Flooding Theory," Paper SPE 89359 presented at the SPE/DOE Fourteenth Symposium on Improved Oil Recovery, Tulsa, USA, pp. 1-16, Apr. 2004.
55. Rivas, O.; Embid, S.; and Bolivar, F., "Ranking Reservoirs for Carbon Dioxide Flooding Processes" SPE Advanced Technology Series J., Volume 2, Number 1, pp. 95-103, March 1992.
56. Gale, J.J., "Opportunities for Early Applications of CO₂ Sequestration Technology", IEA Greenhouse Gas R&D Program File Note, 2003.
57. Caudle, B.H and Dyes, A.B., "Improving Miscible Displacement by Gas-Water Injection", Trans., AIME, pp. 213, 281, 1958.
58. Huang, E.T.S. and Holm, L.W., "Effect of WAG Injection and Rock Wettability on Oil Recovery During CO₂ Flooding", SPE Reservoir Engineering, 119, February 1988.
59. Christensen, J R; Stenby, E H; and Skauge, A., "Review of the WAG Field Experience", paper SPE 71203 presented at the 1998 SPE International Petroleum Conference and Exhibition of Mexico, Villa Hermosa, 3-5 March.
60. Pariani, G.J.; McColloch, K.A.; and Warden, S.L., "An Approach To Optimize Economics in a West Texas CO₂ Flood", JPT, 984; Trans., AIME, 293, September 1992.
61. Surguchev, L.M.; Korbol, R.; and Krakstad, O.S., "Optimum Water Alternate Gas Injection Schemes for Stratified Reservoir," paper SPE 24646 presented at the 1992 Annual Technical Conference and Exhibition, Washington, DC, 4-7 October.

62. Roper, M.K. Jr. and Pope, G.A., "Analysis of Tertiary Injectivity of Carbon Dioxide", paper SPE 23974 presented at the 1992 SPE Permian Basin Oil and Gas Recovery Conference, Midland, Texas, 18–20 March.
63. Bellavance, J.F.R., "Dollardhide Devonian CO₂ Flood: Project Performance Review 10 Years Later", paper SPE 35190 presented at the 1996 SPE Permian Basin Oil and Gas Recovery Conference, Midland, TX, 27-29 March.
64. Farouq Ali, The Unfulfilled Promise of Enhanced Oil Recovery – More Lies Ahead? SPE London Section Presentation, 30 Sept. 2003.
65. Jackson, D.D.; Andrews, G.L.; and Claridge, E.L., "Optimum WAG Ratio vs. Rock Wettability in CO₂ Flooding", paper SPE 14303 presented at the 1985 Annual Technical Conference and Exhibition, Las Vegas, NV, 22-25 September.
66. Quijada, M. G., "Optimization of A CO₂ Flood Design Wasson Field-West Texas" Dissertation, Texas A&M University, August 2005.
67. Gharbi, R. B.C., "Integrated Reservoir Simulation Studies to Optimize Recovery from a Carbonate Reservoir", paper SPE 80437 presented at the SPE Asia Pacific Oil and Gas Conference and Exhibition, Jakarta, Indonesia, 9-11 September.
68. Holm, W. L., 'Evolution of the Carbon Dioxide Flooding Processes', Oil and Gas Journal, 1337, November 1987.
69. Lin, E.C; and Poole, E.S., "Numerical Evaluation of Single-Slug, WAG, and Hybrid Con injection Processes, Dollardhide Devonian Unit, Andrews county, Texas" SPE Reservoir Engineering, November 1991
70. Shedid A. S.; Almehaideb, R.A.; and Zekri, A. Y. "Microscopic Rock Characterization and Influence of Slug Size on Oil Recovery by CO₂ Miscible Flooding in Carbonate Oil Reservoir," The Seventh Annual U.A.E. University Research Conference, UAE.
71. Al-Shehri, D. A., "Carbon Dioxide Minimum Miscibility Pressure for Saudi Arabian Crudes", MS.c. thesis, KFUPM, (KSA), 1987.
72. Rappaport, L A., and Leas, W J, "Properties of Linear Waterfloods", Trans. AIME (198), pp. 139, 1953.

73. Warner, H.R. Jr., "An Evaluation of Miscible CO₂ Flooding in Waterflooded Sandstone Reservoirs" paper SPE 6117 was presented at the Society of Petroleum Engineers AIME 51th Annual Fall Technical Conference and Exhibition held in New Orleans, Oct. 3-6, 1976.
74. Mohanty, K. K., "Development of Shallow Viscous Oil Reservoirs in North Slope" report no. PE-FC26-01EC15186 reported to US development of energy, July, 2003.
75. Kwan, M Y.; Cullen, M P.; Jamieson, P R; and Fortier, R A, "A Laboratory Study of Permeability Damage to Cold Lake Tar Sands Cores", Journal of Canadian Petroleum Technology, Vol. 28 (1), pp. 56-62, Jan-Feb 1989.
76. Jones, F O, "Influence of Chemical Composition of Water on Clay Blocking of Permeability", SPE 631, Journal of Petroleum Technology, 441-446, April 1964.
77. Khilar, K C.; Vaidya, R N.; and Fogler, H S, "Colloidally - Induced Fines Release in Porous Media", Journal of Petroleum Technology, vol. 4, pp. 213 – 221, July 1990.
78. Tang, G.; and Morrow, N R, "Oil Recovery by Waterflooding and Imbibitions – Invading Brine Cation Valency and Salinity", SCA 9911 Proceedings of the International Symposium of the Society of Core Analysts, Golden, CO, August 1999.
79. Filoco, P R.; and Sharma, M M, "Effect of Brine Salinity and Crude-Oil Properties on Oil Recovery and Residual Oil Saturations", SPE 65402, Presented at 1998 SPE Annual Technical Conference and Exhibition, held in New Orleans, LA 27-30 Sept. 1998.
80. Stern, D.: "Mechanisms of Miscible Oil Recovery: Effects of Pore- Level Fluid Distribution," paper SPE 22652 presented at the 1991 SPE Annual Technical Conference and Exhibition, Dallas, 6–9 October.
81. Kremesec, Jr. V.J.; and Sebastian, H.M., "CO₂ Displacements of Reservoir Oils From Long Berea Cores: Laboratory and Simulation Result," Paper SPE 14306, May 1988.

82. Yeh, S.W.; Ehrlich, R.; and Emanuel, A.S.: "Miscible Gas flood Induced Wettability Alteration: Experimental Observations and Oil Recovery Implications," SPEFE (167), June 1992.
83. Rao, D.N.; Girard, M.; and Sayegh, S.G., "Impact of Miscible Flooding on Wettability, Relative Permeability, and Oil Recovery," SPERE (204), May 1992.
84. Bangla, V K.; and Yau, F.; and Hendricks, G R, "Reservoir Performance of a Gravity Stable Vertical CO₂ Miscible Flood: Wolfcamp Reservoir, Wellman Unit", SPE 22898, presented at the 66th annual technical conference and exhibition of the Society of Petroleum Engineers, held in Dallas, TX, Oct 6-9, 1991.
85. Tiffin, D L., and Kremesec, V J, "A mechanistic Study of Gravity-Assisted Flooding", SPE/DOE 14895, presented at the SPE/DOE fifth symposium on Enhanced oil recovery of the Society of Petroleum Engineers and the Department of Energy, held in Tulsa, OK, April 20-23, 1986.
86. Karim, F.; Berzins, T V.; Schenewerk, P.A.; Bassiouni, Z A.; and Wolcott, J M, "Light Oil Recovery from Cyclic Injection: Influence of Drive Gas, Injection Rate and Reservoir Dip", SPE 24336, presented at SPE rocky mountain regional meeting held in Casper, Wyoming, May 18-21, 1992.
87. Thomas, J.; Berzins, T. V.; Monger, T. G.; and Bassiouni, Z. A., "Light Oil Recovery from Cyclic CO₂ Injection: Influence of Gravity Segregation and Remaining Oil", SPE 20531, presented at the 65th Annual Technical Conference and Exhibition of the society of petroleum Engineers held in New Orleans, LA, September 23-26, 1990
88. Raimondi, P.; and Torcaso, M.S., "Mass Transfer between Phases in a Porous Medium: A Study of Equilibrium", SPEJ (51), March 1965.
89. Righi, E.F.; Royo, J.; Gentil, P.; Castelo, R.; and Monte, A.D. "Experimental Study of Tertiary Immiscible WAG Injection", Paper SPE 89360, SPE/DOE Symposium on Improved Oil Recovery, Tulsa, Oklahoma, 17-21 April 2004.
90. Mangalsingh, D.; and Jagai, T., "A Laboratory Investigation of the Carbon Dioxide Immiscible Process", Paper SPE 36134, SPE Latin America/Caribbean Petroleum Engineering Conference Port-of-Spain, Trinidad, 23-26 April 1996.

Engineer: Ali Suleman Al-Netaifi

KSA, Riyadh

P.O. Box: 90582 Riyadh 11623

Tel. (Office): +966-1-4676883

Tel. (Home): +966-1-4561396

Tel. (Mobil): +966-555244970

Fax : +966-1-4674422

E-mail: Notaiify@ksu.edu.sa

ملخص الرسالة

إن الزيادة في إنتاج الزيت الخام بطريقة الغمر الإمتزاجي تحدث عن طريق ثلاثة آليات. هذه الآليات تكمن في إزاحة الزيت بواسطة المذيب (غاز ثاني أكسيد الكربون) عبر إمتزاج للغاز بالزيت الخام، وإنتفاخ الزيت الخام، وتقليل لزوجة الزيت الخام.

لتقييم أداء عمليات الغمر المتتابع للغاز والماء تم إجراء تجارب معملية على عينات من الصخر الرملي ذات أطوال مختلفة (2قدم، 4قدم) باستخدام محاليل ملحية مائية ذات تراكيب وتراكيز مختلفة، وإستخدام زيوت مختلفة (الديكان الطبيعي، والزيت السعودي الخام الخفيف، والزيت السعودي الخام متوسط الكثافة). ولقد تم دراسة تأثير كلا من نوعية ضخ الغاز (في حالة الغمر المتتابع للغاز والماء، وفي حالة الغمر المتواصل للغاز)، ونسبة ضخ الماء للغاز المتتابع، وحجم الجبهة المحقنة للغاز والماء، ونوع الزيت المستخدم، وإتجاه حقن الغاز للعينة الصخرية (عمودي و أفقي)، وطول العينات الصخرية المستخدمة على معامل الإنتاج للزيت الخام ومعامل الإنتاج الثلاثي للزيت الخام بالغاز. وبالإضافة إلى ذلك تمت مقارنة إنتاجية كل من الغمر المتتابع للغاز والماء كعملية ثنائية وكعملية ثلاثية (لحقن الغاز) عند نفس الظروف.

لقد أثبتت نتائج تجارب الغمر الإمتزاجي الثلاثي للزيت الخام للغاز أن نسبة الماء للغاز 2:1 وحجم الجبهة المحقنة للغاز والماء 0,2 هما أفضل عوامل للغمر المتتابع للغاز والماء حيث أدت هذه العوامل إلى أفضل معامل إنتاج وأفضل معامل إنتاج ثلاثي لزيت الخام بالغاز. وبالتالي فإن كمية كبيرة من الغاز المحقون يستهلك خاصة في المراحل الأولى لعملية الحقن.

ولقد ثبت أن كلا من معامل الإنتاج ومعامل الإنتاج الثلاثي للزيت الخام بالغاز يقل عندما تزيد كثافة الزيت (أي عندما تنخفض API) ويعتقد أن هذا يرجع إلى تغير خاصية تبلل الصخر الرملي، وأيضاً إلى سرعة خروج الغاز نتيجة إلى إختلاف اللزوجة ما بين الزيت الخام والغاز (Viscous Fingering). وثبت أن معامل الإنتاج النهائي للزيت الخام يتساوى عند إستخدام محاليل مائية مختلفة التركيب والتركيز إلا أنه قد يحدث بعض التأخير في معامل الإنتاجية باستخدام المحلول المائي منخفض الملوحة. وهذه النتيجة أدت إلى زيادة معامل الإنتاج الثلاثي للزيت بالغاز وأيضاً تقليل معامل إستهلاك غاز ثاني أكسيد الكربون نسبياً في حالة زيادة ملوحة المحلول المائي.

إن معامل إنتاج الزيت الخام في حالة الغمر الإمتزاجي المتتابع للغاز والماء في الإتجاه العمودي يكون أقل نسبياً من حالة الغمر المتتابع للغاز والماء في الإتجاه الأفقي. وفي حالة مقارنة نتائج الغمر الإمتزاجي المتتابع للغاز والماء بإستخدام عينات صخرية مختلفة الطول (2قدم، 4قدم) وجد أن معامل الإنتاج يتساوى في كلتا الحالتين، إلا أنه لوحظ بعض التأخير في معامل الإنتاج في حالة إستخدام العينات الصخرية القصيرة (2قدم).

إن معامل الإنتاج في حالة الغمر الإمتزاجي المتواصل بغاز ثاني أكسيد الكربون وبإسخدام الديكان الطبيعي يكون أفضل من معامل إنتاج الزيت الخام في حالة الغمر الإمتزاجي المتتابع للغاز والماء، ويرجع ذلك إلى أن صخور البيريا المستخدمة في هذا البحث معروف عنها أنها شديدة التبلل بالماء. وبالإضافة إلى أن الزيت المستخدم (الديكان الطبيعي) أيضاً معروف عنه إنه غير مبلل للصخر، لذلك هذه النتائج تتفق تماماً مع الدراسات السابقة التي تشير إلى كفاءة الغمر المتواصل بالغاز في الأوساط الصخرية المبللة بالماء، بينما هذه الطريقة تحتاج إلى ضخ كميات كبيرة من الغاز لذلك تعتبر غير إقتصادية. وعندما طبقت نفس المقارنة السابقة ولكن بإسخدام الزيت السعودي الخام الخفيف وجد أن معامل إنتاج الزيت الخام في حالة الغمر المتتابع للغاز والماء هو الأعلى، وهذا التناقض في النتيجة ما بين مقارنة الغمر المتواصل بالغاز والغمر المتتابع للغاز والماء في حالة إسخدام الزيت السعودي الخام الخفيف والديكان الطبيعي، يرجع إلى أن تواجد الزيت الخام الذي من الممكن أن يغير خاصية تبلل الصخر بحيث تصبح أقل قابلية للتبلل بالماء وأكثر قابلية للتبلل بالزيت وهذا بدوره يمنع إحتباس الماء أثناء الغمر المتتابع للغاز والماء.